Expertise
and insight
for the future

Edvard Nyman

Design of a Semiconductor Substrate Heating Station

Metropolia University of Applied Sciences

Bachelor of Engineering

Mechanical Engineering

Bachelor's Thesis

21 May 2019

Author Title Number of Pages Date	Edvard Nyman Design of a Semiconductor Substrate Heating Station 50 pages 21 May 2019
Degree	Bachelor of Engineering
Degree Programme	Mechanical Engineering
Professional Major	Machine Automation
Instructors	Pekka Soininen, Head of Technology Antti Liljaniemi, Senior Lecturer

The objective of this thesis was to investigate the operation of a wafer heating module. The module was a part of an atomic layer deposition (ALD) cluster tool and had the purpose of pre-heating semiconductor wafers to the target process temperature prior to their insertion into the ALD reaction chamber.

The module was intended to process large wafer lots in rapid succession, but was observed to be incapable of consistently and repeatably heating each wafer in the lot to the target temperature.

A series of tests were conducted to establish an understanding of the heater's operating principles and the physical phenomena occurring inside the module in order to find the cause of the problem.

In addition, a literature survey was conducted to find examples of designs for similar pieces of equipment and consequently to compose a theoretical understanding of the heater's function.

Based on the findings of the investigation and the literature survey, a new heater design was created in which the deficiencies of the previous design were rectified.

Keywords	Semiconductors, rapid thermal processing, atomic layer deposition, pyrometry, vacuum technology

Tekijä Otsikko Sivumäärä Aika	Edvard Nyman Puolijohdekiekkojen lämmitysaseman suunnittelu 50 sivua 21.5.2019
Tutkinto	Insinööri (AMK)
Tutkinto-ohjelma	Konetekniikka
Ammatillinen pääaine	Koneautomaatio
Ohjaajat	Head of Technology Pekka Soininen Lehtori Antti Liljaniemi

Insinöörityön tavoitteena oli parantaa erään kiekonlämmitysaseman toimintaa. Asema oli osa atomikerroskasvatukseen (ALD) suunniteltua klusterikonetta, ja sen tarkoitus oli esilämmittää puolijohdekiekkoja prosessilämpötilaan ennen niiden vientiä ALD-reaktiokammioon.

Asema oli tarkoitettu suurten kiekkoerien käsittelyyn, mutta sen havaittiin olevan kykenemätön lämmittämään kokonaisia eriä kohdelämpötilaan toistettavasti ja luotettavasti.

Työssä suoritettiin sarja kokeita, joiden tarkoituksena oli muodostaa käsitys lämmittimen toimintaperiaatteista sekä sen sisällä tapahtuvista fysikaalisista ilmiöistä ongelman syiden löytämiseksi.

Lisäksi työn osana tehtiin kirjallisuusselvitys, jonka tarkoituksena oli löytää esimerkkejä samantyyppisistä laitemalleista ja siten muodostaa teoreettinen käsitys lämmittimen toiminnasta.

Kokeiden ja kirjallisuusselvityksen löydösten perusteella suunniteltiin uusi lämmitysaseman malli, jossa edellisen mallin puutteet oli korjattu.

Avainsanat	Puolijohteet, rapid thermal processing, atomikerroskasvatus, pyrometria, tyhjiötekniikka

Contents

List of Abbreviations

ALD	Atomic layer deposition.
TFEL	Thin film electroluminescent (display).
IC	Integrated circuit.
CVD	Chemical vapor deposition.
RTP	Rapid thermal process(ing/or).
IR	Infrared.
NIR	Near-infrared.
PWM	Pulse width modulation.
PID	Proportional-integral-derivative (controller).

1 Introduction

In the last two decades, single wafer processing has almost entirely replaced batch processing in semiconductor manufacturing. The transition to the single-wafer approach has been facilitated by increasingly stringent demands placed on integrated circuits by the market, driving manufacturers to adopt production processes with a higher degree of precision and controllability [1].

The advantages of the single-wafer approach are, however, offset by lowered throughput. This has necessitated the development of other approaches for increasing processing volume. One such approach is the cluster tool, in which wafers are rapidly cycled through various successive processes within the same processing unit. This allows for time-efficient processing of large wafer lots without the need to process a lot as a single batch [2].

This thesis covers the development process of a wafer heating module for an Atomic Layer Deposition (ALD) cluster tool.

The project was commissioned by Beneq Oy, a nanotechnology company based in Espoo, Finland. The company's two main lines of business are the manufacturing of ALD equipment and thin film electroluminescent (TFEL) displays, the latter being sold under the brand name Lumineq [3]. Additionally, Beneq markets thin film coating services as a means for companies and organizations to outsource thin film production [4-5].

Though originally developed specifically as a TFEL production method, ALD today has a wide range of applications, particularly in the semiconductor and microelectronics industries. Other applications include optical and anti-reflective coatings for lenses and photovoltaic panels, protective coatings for sensitive instruments and bio-inert coatings for biomedical devices [6]. While in many other fields ALD is still a novel technology, it has been considered an established, mainstream process in the microelectronics industry for over a decade [7].

Recently, Beneq has recognized the necessity of being able to offer equipment for large-scale wafer production, and the development of a volume-production capable ALD tool

model has been ongoing for some time. The project covered in this thesis represents one facet of this wider development process.

1.1 Problem statement

Prior to the start of this project, several prototype cluster tool designs had already been produced by Beneq. The basic design includes, as one of the cluster's process modules, a heating station for rapid pre-heating of wafers prior to their insertion into the main reaction chamber.

The heating modules in the first pilot tools were supplied by an outside equipment vendor, who also supplies the wafer handling system used in the clusters. As lot sizes were increased between the consecutive tool designs, it became apparent that the supplied heating module design was incapable of processing large lots of wafers in a reliable manner.

The central problem was temperature readings becoming increasingly erroneous after each consecutive heating. When processing large lots of wafers, the error would compound until the initial wafer temperature reported by the sensors would be very close to the target temperature. As the heating was controlled using closed-loop feedback from the temperature sensors, this meant that heating times would steadily decrease until the heating elements would no longer turn on at all. Other problems included differences in the heater's behavior when processing different substrates as well as overshooting of the target temperature.

The heating modules were designed at Beneq's request and are not part of the supplier's standard product range. Thermal processing is also outside of the supplier's core competence area, and the supplier has neither been able to provide workable solutions to the problems with the design nor expressed a strong inclination to carry out further development.

Although rapid thermal processing equipment for various different microfabrication processes exists, seemingly none have been developed specifically for ALD applications, and processing equipment suitable for this purpose is not readily available on the market.

Thermal processors are also typically sold as integrated parts of self-contained processing equipment rather than separate modules [8].

Reliable heating of the wafers is critical for achieving the throughput targets specified for the cluster tools in general as well as the units currently in engineering and production. There is hence a need to resolve the problems affecting the design within a rapid schedule. Together, these factors necessitate the development of a new design to be carried out in-house.

1.2 Purpose and objective

The purpose of this thesis is to ascertain which factors cause the distortion of temperature readings during wafer processing in the previously described heating module and to establish what manner of modifications to the module's physical design and/or control scheme are necessary to eliminate the distortion.

The primary objective is hence to develop a new design for the heating module in which the immediate problems affecting the current design have been resolved. The new design should work reliably enough to enable the cluster's throughput and quality targets to be reachable. This requires accurate wafer temperature measurement within the specified temperature range as well a process control scheme sufficiently precise to prevent significant overshooting of the target temperature.

A secondary objective is to gather and document the theoretical background relevant to the heater's design for later use in the company. This is to ensure that there is sufficient and readily available information to draw from in the case that there is a need develop the design further for more demanding applications.

1.3 Methods

The first part of this thesis is a literature survey, summarizing relevant findings from scientific and educational literature relating to the topic of this thesis. The purpose of this is to establish a sufficient theoretical understanding of the heater's function, to examine some

commonly used methods of temperature measurement and control, and to find examples of functional wafer heating equipment designs.

The second part is an investigation into the heater's function, in which a series of tests are performed with the heater in order to quantify the degree of the measurement error and to record how substrate heating is affected by different pre-conditions and process parameters.

The third part is an analysis of the investigation's results utilizing the theory gathered in the first phase. Finally, a revision of the heating station's design is carried out based on the conclusions of the analysis.

2 Theoretical background

2.1 Semiconductor manufacturing

All modern electronics are based on semiconductor technology.

Semiconductors derive their name from the fact that the conducting properties of a semiconductor material can be altered by introducing impurities into the material's crystal structure – a process known as doping. Areas of a semiconductor's surface can be selectively altered to create electrically conductive patterns on the substrate's surface, thus creating an integrated circuit (IC) [9].

The manufacturing process of a microchip begins from substrate refinement and wafer manufacturing. A wafer (pictured in figure 1) is the basic stock material used in the IC industry. The terms *wafer* and *substrate* are used mostly interchangeably to refer to the semiconductive material on which an IC chip is fabricated on. Silicon is by far the most common substrate used in the industry. Some of the other substrate materials include germanium (Ge), gallium arsenide (GaAs), silicon compounds such as silicon carbide (SiC) and various special grades of glass [9, 11].

Figure 1. Variously sized silicon ingots (top) and wafers (bottom) [10].

The first phase in the manufacture of wafers is the production of a purified, single-crystal ingot. An ingot is made by growing it around a small, monocrystalline sample (called a

seed) of the element or compound by immersing it in a pool of the molten substance until a solid block in the desired dimensions is obtained. The ingot is then sliced into thin discs, which are mechanically and chemically polished. The result is a monocrystalline slice of a very pure semiconductive material.

Due to the way ingots are formed during the production process, the most common shape for a semiconductor wafer is a round disc. For special applications, the wafers may be fashioned further into other shapes, such as rectangles, squares and pseudosquares. Additional processing naturally increases the wafer's cost. This is a consideration since manufacturers typically source their wafers from outside companies that specialize in wafer production.

Wafer sizes in the semiconductor industry are highly standardized. Currently wafers come in sizes of 100, 150, 200, and 300 mm [12]. Additionally, the industry is in the process of adopting 450 mm wafers; this development has, however, been slow due to technical challenges related particularly to automated wafer handling [13].

The fabrication of a circuit on the wafer is a multiple-step process that includes a wide variety of different procedures. Depending on the complexity of the circuit, the fabrication process may include hundreds of steps, and it is common for the entire fabrication process from a bare wafer to an encased microchip to take from several weeks to a month or even longer. Many of the individual processes are repeated several times in order to create a layered structure on the substrate surface.

The basic tool used for fabricating patterned layers is a process called photolithography. In photolithography, the wafer is coated with a light-sensitive substance called a photoresist. The resist is then exposed selectively to UV light through a patterned mask. Immersing the wafer in a chemical bath etches away the exposed areas while retaining the unexposed ones. This leaves the wafer covered with a patterned layer which covers some areas of the wafer while leaving others exposed. The exposed areas of the underlying layer can then be treated using various additive, subtractive or transmutative techniques to create structures of the substrate or to alter its properties. After the treatment, the remaining photoresist is removed.

A typical additive process is deposition, where a material layer is “grown” on the substrate’s surface. One example of a deposition method is chemical vapor deposition (CVD), in which the surface is exposed to one or several gaseous-phase chemicals which react with the substrate and/or one another, forming a film on the substrate’s surface.

Etching is a typical subtractive technique. It can be performed either by using a chemical solution or plasma. Of these two, plasma etching (also known as dry etching) is more commonly used by large IC manufacturers due to its higher precision.

Doping, as mentioned before, is the most common way of altering a semiconductor’s material characteristics.

Doping can be done using multiple techniques, such as diffusion and ion implantation. The substrate gains either a negative or positive charge depending on which dopant is used. A doped semiconductor substrate is hence referred to as n-type or p-type, respectively.

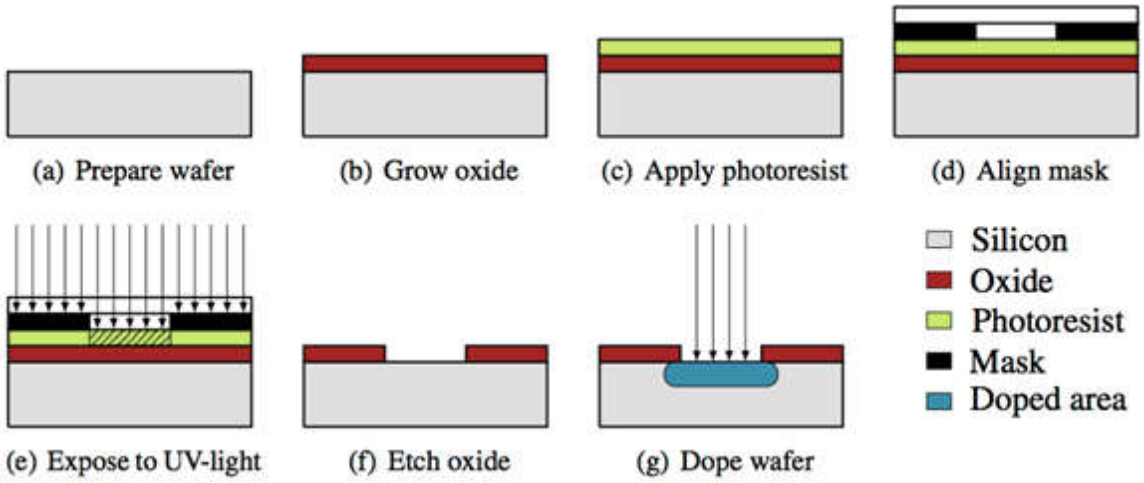

Figure 2. An example of the fabrication of a single layer on a substrate’s surface [14].

A simplified step-by-step schematic showing a deposition followed by photolithography, etching and doping is shown in figure 2. A real-life example of a microscopic structure created using repeated application the described techniques can be seen in figure 3.

After all layers have been fabricated, the wafer is coated with a final protective layer. The wafer is then cut into square-shaped dies, each of which contain a single circuit on their surface. The size of a die can vary between 1 mm x 1 mm and 10 mm x 10 mm (or even larger) depending on the circuit's footprint [15 – 16]. An example of how a wafer is partitioned is shown in figure 4.

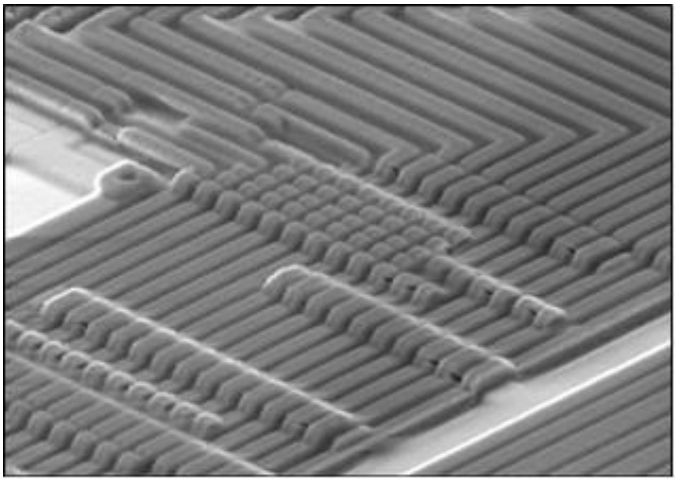

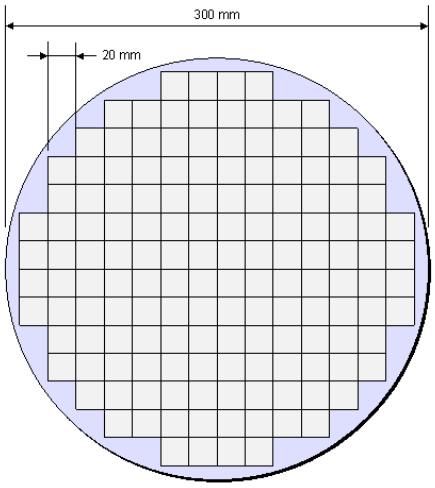

Figures 3 and 4. An example of a microscopic structure on a chip's surface (left) [17]. Die mapping on a 300 mm wafer (right) [18].

As touched upon in the introductory chapter, an increasingly common approach to sequencing the steps in an IC fabrication process is the cluster tool, in which a wafer handling robot sequentially cycles wafers through a number of successive processes inside a single multiple-process machine. This is in contrast to processing wafers one fabrication step at a time in dedicated single-process machines, which was the standard operating model in the industry's starting decades. The cluster approach speeds up the fabrication process significantly, for which reason it is becoming an increasingly common way of circuit fabrication despite the high costs of the equipment involved [19].

This thesis focuses on the equipment used to conduct one specific step in the larger fabrication process of an IC chip, namely deposition using a specific deposition technique.

2.2 Atomic layer deposition

Atomic layer deposition is, as its name implies, a deposition method in which a substance is deposited on a surface one monolayer at a time. It is usually regarded as a type of chemical vapor deposition technique.

The process works by sequentially introducing a number of chemically volatile substances (called *precursors* or, more generically, *reactants*) to the reaction area. The substances react to form a compound on the substrate's surface. Most ALD processes use two reactants, although three or more are also possible. The reactants can be both pure elements and chemical compounds, or any chemically viable combination of the two.

In contrast to more conventional CVD techniques, in ALD the reactants are never simultaneously present in the reaction area; the previous reactant is flushed out before the next is introduced.

In today's semiconductor industry, ALD has become key technology in facilitating the downscaling of microelectronics. As the technique makes it possible to control the thickness of deposited films on the level of single-molecule layers, very small structures can be constructed with a degree of precision not afforded by any other deposition method.

One of the characteristic features of ALD is that the process cycles are self-terminating. Once all available surface area that the reactants can bond with has been occupied, bonding ceases. The self-terminating nature of the process cycles enables layers to be grown to a thickness of a single molecule [20].

ALD has been historically known by several different names, including Atomic Layer Epitaxy (ALE), Molecular Layering (ML) and Molecular Layer Deposition (MLD). The current name became established in the 1990s. Publications older than this may refer to the process by any of the aforementioned names.

The process itself was discovered by Tuomo Suntola, originally under the name of ALE, in Finland in the early 1970s. The first successfully facilitated ALD reactions were based on elemental reactants – particularly zinc and sulfur, which produced zinc sulfide, an electroluminescent compound. The early work of Suntola's team hence focused on

electroluminescent thin films, a practical application of which were TFEL displays. TFEL development was a driving factor of early ALD research. The effort to develop higher quality EL films eventually drove the researchers to switch to compound reactants, which expanded the possibilities of ALD significantly.

Suntola's team disclosed their work to the public in 1980, and the commercialization of TFEL displays began in 1983. Research into other applications, such as photovoltaic panels and, more importantly, semiconductors began some years later. Simultaneously, research teams elsewhere in the world, particularly in the US and Japan, also began investigating ALD. Major semiconductor manufacturers began to show interest in the process in the 1990s. Today, the process is considered a mainstay in the semiconductor industry, and, as mentioned earlier, a significant factor in the continuing miniaturization of electronics [21].

Suntola has since (in 2018) received the Millenium Technology prize, awarded by Technology Academy Finland for impactful technological innovations, for his work on ALD [22].

The process of growing a single material layer in a two-reactant process consists of four steps:

1. The first reactant is introduced in gaseous form into the reaction area (i.e. process chamber). Reactant molecules bond with the naked substrate or pre-existing layer of film until all available surface area is occupied.

2. Excess reactants and any byproducts of the previous reaction are flushed out of the reaction area using an inert gas (typically nitrogen).

3. The second reactant is introduced into the reaction area. Reactant molecules bond with the layer formed by the first reactant to create a compound.

4. Excess reactants and byproducts are flushed out of the reaction area, leaving a single-molecule layer of chemical compound created from the two reactants.

These steps are depicted in figure 5.

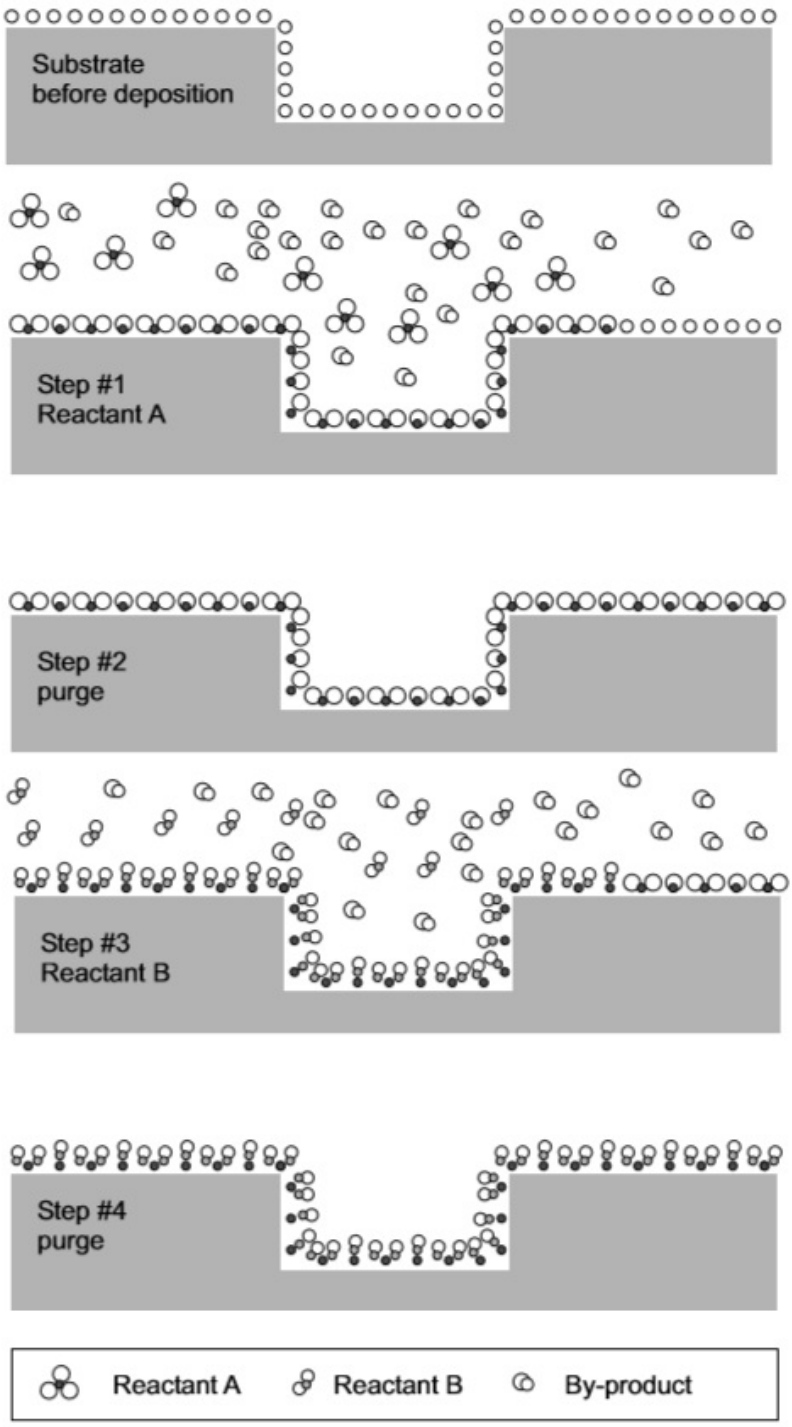

Figure 5. Schematic illustration of the mechanics of the ALD process [20].

For example, in one common and typical ALD process, the first reactant, trimethylaluminium ("TMA") is adsorbed by the substrate surface, producing no byproducts. The second reactant, water, then reacts with the TMA to form an aluminium oxide film and gaseous methane as byproduct.

Together, the steps described above form a single *cycle*. Cycles are repeated as many times as required to grow a film of the desired thickness. The number may vary between less than a hundred to several thousand. The processing time increases linearly based on the number of cycles. Deposition of a single reactant preceding or following that of the other is usually referred to as a *half-cycle*.

Conditions inside the reaction area are carefully controlled to ensure that the reaction occurs in the desired manner. Reactions are conducted under vacuum to ensure that only substances involved in the desired process are present in the reaction area. This keeps reactants from being consumed in undesired reactions with e.g. oxygen, as well as impurities from forming in the deposited film. The reaction chamber parts are treated to remove any impurities for the same reason.

Process variables must likewise be precisely controlled. Temperature of the substrate and the reactants must be at a specific values for the necessary chemical reactions to occur. The substrate must have a uniform heat profile, as temperature disuniformities on the substrate's surface will result in uneven film growth [20].

In contrast to a number of other processes used in IC fabrication, ALD is, due to the nature of the process, well suited for batch processing. Coating a batch of wafers takes no more time than coating a single wafer, provided that the gas distribution parts in the chamber are scaled accordingly to provide a larger reactant flowrate. Wafer throughput can therefore be substantially increased by processing multiple wafers at a time.

2.3 Rapid thermal processing

Rapid thermal processing (RTP) is a blanket term for a group of semiconductor manufacturing processes characterized by the transfer of high amounts of thermal energy to a wafer in a short period of time. The term can be used to refer to rapid thermal annealing, oxidation, nitration, chemical vapor deposition, as well as any combinations of these processes [23].

The exact definition of RTP is somewhat nebulous, but it is generally agreed that RTP is a single-wafer process with fast heating and cooling times where the wafer is thermally isolated from the process chamber [24]. The latter requirement essentially means that the

wafer is heated in a contact-free manner under vacuum. The primary (and ideally, sole) means of energy transfer to the wafer in RTP is hence radiation.

The defining characteristic that sets RTP apart from conventional thermal processing – usually conducted in a batch furnace – is that the wafer never reaches thermal equilibrium with its surroundings. In batch furnace processing, the furnace is first heated to the wafers' target temperature. Wafers are then inserted into the furnace, where their temperature slowly rises to match that of their surroundings. Conversely, in RTP, the heat source is always substantially hotter than the wafer [24]. This difference in temperature between the heat source and the wafer is what facilitates rapid heating.

Though the equipment can be used solely for wafer heating, RTP is usually thought of as a phased process where the heating of the wafer to the target setpoint is followed by a processing phase, in turn followed by the cooling of the wafer to ambient temperature. Commercial RTP systems are therefore designed to enable one or more IC fabrication processes to be performed in them.

An RTP system can be broken up to the following basic components: heat source, process chamber, temperature measurement instrumentation, controller and wafer transport system [25]. The most commonly employed types of heat sources, chamber designs and temperature sensors will be covered in the following subchapters. Control will be covered only briefly due to the complexity of the subject. Wafer transport systems will not be covered as they have no relevance for the research problem addressed in this thesis.

2.3.1 Heat sources

Heat sources used in RTP systems can be broadly categorized into three groups: coherent light sources, incoherent light sources and continuous resistive radiation sources.

Each of these heat sources emit either all or a significant portion of their radiation in the infrared spectrum. Silicon, which is the most common semiconductor substrate, is the most absorptive of IR radiation in the near-infrared region (specifically around 1.1 µm). For this reason, RTP heat sources are designed to output their peak radiation around this wavelength range [25].

The term coherent light source essentially refers to lasers. The earliest form of RTP was pulsed laser irradiation, used mostly for annealing [25]. The technique works by targeting closely arranged spots on the wafer's surface with a laser. By using multiple lasers and by timing the successive pulses sufficiently rapidly, the wafer's temperature can be raised across its entire surface in a fairly uniform fashion. However, sequential spot-exposure of this sort is more liable to causing surface deformities than blanket irradiation, which is of particular importance when wafers with surface structures are being processed. For this reason, laser pulsing is much less common today [26].

Incoherent light refers to unfocused light such as that emitted by a lamp. When used to heat wafers, the wafer's surface is exposed to the light uniformly and simultaneously across its entire surface, as opposed to the spot-exposure induced by laser-pulsing. The two types of incoherent light sources commonly used in RTP systems are tungsten-halogen lamps and arc lamps.

The tungsten-halogen lamp consists of a resistively heated tungsten filament contained inside a hollow quartz casing, typically in the shape of a tube. A halogen gas is used as the fill gas. When the lamp is on, the filament's temperature reaches around 2000 °C, while the quartz tube typically heats up to 400 °C.

Arc lamps similarly consist of an outer casing, usually made of quartz or a heat-resistant glass (such as Pyrex). Arc lamps use noble gases as the fill gas instead of halogens. In place of a filament, the lamp has electrodes at each end, which ignite an arc in the gas when voltage is applied. The outer casing of an arc lamp is typically water cooled due to the lamp's high energy output.

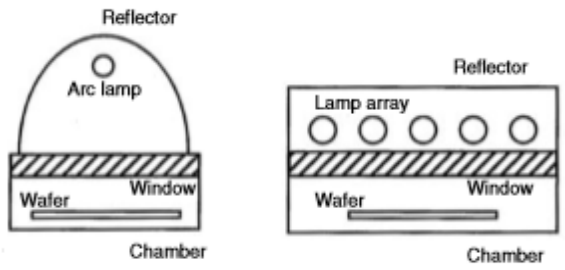

Figure 6. Simplified schematics of RTP chambers heated by a single arc lamp (left) and an array of tungsten-halogen lamps (right) [28].

The irradiative power generated by an arc lamp is substantially higher than that generated by a halogen lamp. Due to this, systems employing an arc lamp as the heat source typically only use a single lamp, paired with a reflector designed to distribute the radiation evenly to the wafer. Figure 6 demonstrates such a design.

In contrast, tungsten-halogen lamps are commonly employed in lamp arrays consisting of multiple lamps [25]. Figure 7 presents a collection of common lamp array designs. The first three are axisymmetric arrays. The first and second array are composed of spot lamps arranged in concentric heating zones and a honeycomb pattern, respectively. The third is composed of linear lamps. The fourth is a cross-grid array composed likewise composed of linear lamps [6].

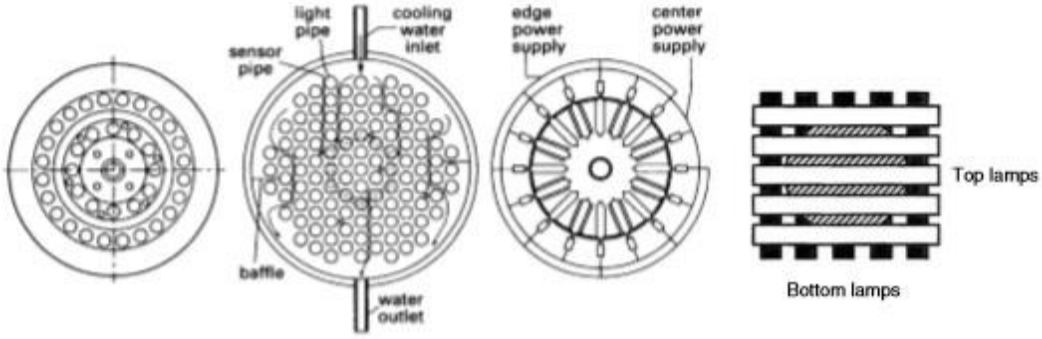

Figure 7. A collection of lamp array designs [27, 28].

The advantage of using multiple spot lamps is that variable amounts of energy can be delivered to different areas of the wafer, which enables better control over temperature uniformity. The cross-grid design, in contrast, delivers the same amount of radiation across the entire irradiated area.

In contrast to light sources, which are turned on for the duration of the heating operation and then disengaged, continuous resistive radiation sources are kept continuously “on”, and the wafer’s exposure to the radiation is regulated in other ways. Two examples of such heat sources are the planar graphite sheet and the silicon carbide bell jar.

The former is a simple sheet of graphite which is resistively heated to a temperature range of 1000 – 1400 °C. The temperature is constant across the entire sheet. Transfer of thermal energy is determined by time of exposure, which in turn is regulated by a shutter between the sheet and the wafer [29].

The bell jar is essentially a hollow upturned vessel with an open bottom with the resistive elements placed in contact with the closed end. This causes the bell jar to have a temperature gradient across its structure. A wafer is inserted into the jar using a lift mechanism. Since radiation exposure is determined by the wafer's distance from the hot end, the wafer's temperature can be regulated by its positioning inside the enclosure using the lift. Figure 8 demonstrates the principle.

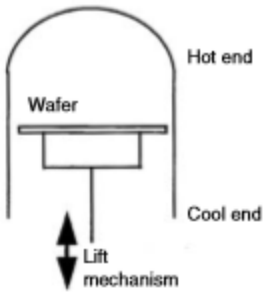

Figure 8. A simplified schematic of a bell jar heater [28].

The wavelength of the radiation emitted by these two materials is variable and dependent on the material's temperature. This enables fairly precise control over the range of radiation which the wafer is exposed to [25].

2.3.2 Chamber design

Commercial RTP systems can be divided into three types based on chamber design. These three designs are the cold wall, warm wall and hot wall chambers.

The basic structure common to all three types of RTP chambers consists of a vacuum-proof outer metal housing, commonly manufactured from a metal alloy such as aluminium or stainless steel. The wafer is held in place at the chamber's centre with holding pins or a tray so that it is not in contact with the chamber walls. Heat sources may be positioned on one or both sides of the wafer. If chemical processes are conducted concurrently to heating, the chamber additionally has an inlet and outlet for gas flow.

Hot wall designs are those in which the chamber wall itself acts as the system's heat source. An example of such is the SiC bell jar design described previously. The two other types use incoherent light sources to heat the wafer.

Cold wall designs are characterized by a water-cooled chamber housing. The purpose of cooling is to keep the chamber at a low enough temperature to prevent the inner wall from acting as a secondary radiation source. The chamber's inner surfaces are also commonly electropolished or coated with a reflective material to lessen the rate of radiation absorption by the walls.

Warm wall designs additionally contain a secondary enclosure inside the outer chamber housing which atmospherically separates the wafer from the rest of the chamber space. This allows for gas reactions such as CVD to be conducted without the reactants coming into contact with the chamber walls, which prevents metal contamination. A typical material for the wafer enclosure is quartz, which is permeable to NIR radiation and also chemically fairly inert. The inner enclosure is air-cooled (as opposed to water-cooled like the outer housing), which is where the design's name is derived from [25].

An example of a warm wall RTP chamber is presented in figure 9. The figure contains all the basic design features of an RTP chamber.

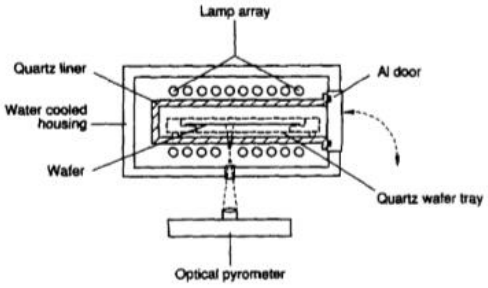

Figure 9. A warm wall RTP chamber with double-sided heating [3].

Depending on which processes the system is designed for, the chamber may include additional design features. For example, a system designed for rapid thermal CVD will commonly have features intended to improve temperature uniformity, and consequently the quality of the deposited film, such as temperature guard rings around the wafer's edges or a rotating wafer holder [30].

2.3.3 Temperature measurement

The principal method of temperature measurement used in RTP systems is pyrometry. This is a non-contact method based on measuring the intensity of radiation emitted by an object at a specific wavelength or wavelength range. As all objects which have a temperature above absolute zero emit infrared radiation, IR wavelengths can be used to determine an object's temperature.

The primary advantage of pyrometry over other temperature measurement methods in the context of RTP is that it is non-contact. This is critical in RTP since it prevents contamination and does not require any preparation steps. Other advantages of pyrometry include fast response time and suitability for measuring very high temperatures [31].

All materials have three intrinsic spectral properties: emissivity (ε), transmissivity (τ) and reflectivity (ρ). Emissivity indicates how strongly an object emits radiation, transmissivity indicates how much radiation passes through the object, and reflectivity indicates how much radiation is reflected off the object's surface. Each of these properties have a value between 0 and 1 (in the case of τ and ρ, often expressed as a percentage). The magnitude of each property is dependent on the two others such that ε + τ + ρ always equals 1. Therefore, for example, if emissivity increases and reflectivity stays the same, then transmissivity must decrease [32].

Furthermore, a material's spectral properties vary between wavelengths. For example, glass is transparent to visible light but opaque to IR light past a certain wavelength. Conversely, some optical materials such as germanium are not transparent to visible light, but transmit IR radiation well [33].

The spectral properties of the measured substrate as well as all of the materials used in the construction of the RTP chamber must be properly understood to choose the correct measuring range for a pyrometer. A complicating factor in measuring the temperature of silicon is that its properties are highly dependent on a large number of factors. Besides exhibiting variable emissivity across the IR spectrum, its spectral properties also change depending on temperature. Figure 10 demonstrates the emissivity of pure, uncoated silicon in the IR spectrum at different temperatures.

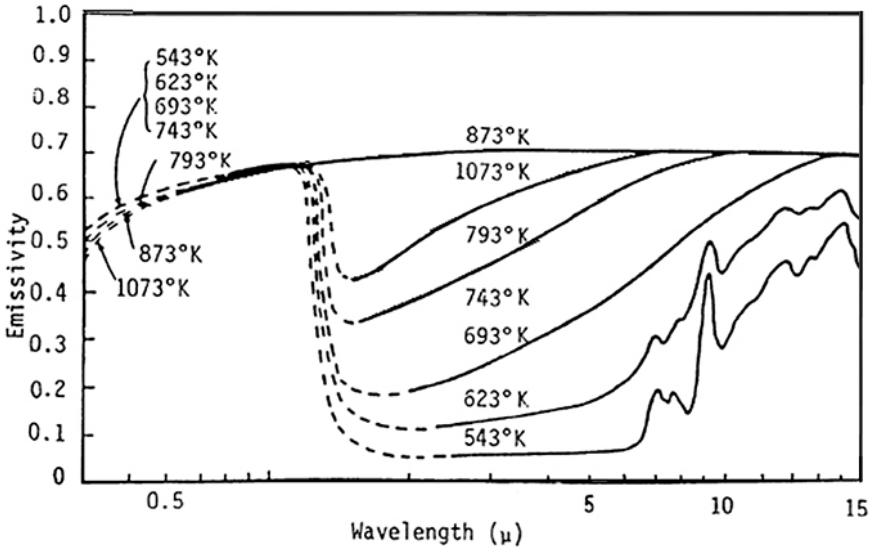

Figure 10. Spectral emissivity of silicon in various temperatures [34].

By assuming that the reflectivity of a silicon wafer stays the same, silicon's transmissivity can be deduced from the same figure. It can hence be observed from the figure that silicon behaves as an opaque material with an emissivity of 0.7 in temperatures of over 600 °C. In lower temperatures, it is almost fully transparent in most of the middle infrared range. [36]

To obtain effective measurements from the substrate, the pyrometer's spectral band must be chosen so that it coincides with a range where the substrate exhibits high emissivity. In silicon's case, this depends on the temperature of the process. The most common wavelengths used for pyrometry in RTP systems, where the processing temperatures are often very high, fall between 0.95 and 4.5 μm. Shorter wavelengths are preferred since they are known to minimize emissivity errors during measurement [37].

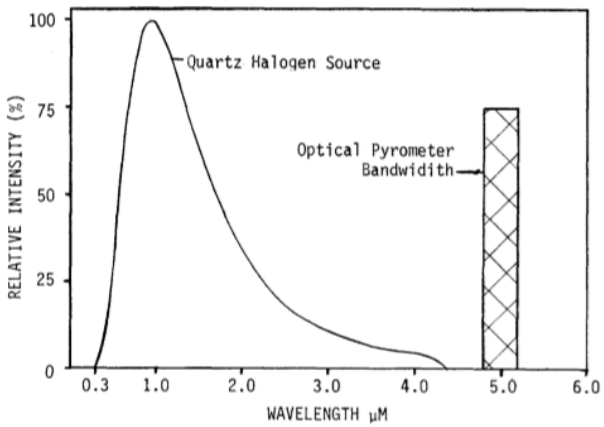

Figure 11. The spectral distribution of a tungsten-halogen lamp and the measurement range of a pyrometer [32].

Engineering and design considerations may however further rule out certain wavelength ranges. For example, in a system utilizing an incoherent light source, the pyrometer's spectral band must me selected so that it falls entirely outside of the range in which the light source emits radiation. This principle is demonstrated in figure 11 [32].

The emissivity value of the measured substrate must also be known exactly as pyrometers require their emissivity setting to match the emissivity of the target to obtain accurate readings. While the spectral properties of the most common substrates are fairly well known, these are only applicable to pure, undoped and uncoated wafers. Calculating the emissivity of coated or otherwise surface-processed wafers is mathematically a highly complex task and it cannot be effectively done without the use of advanced computer software [38].

The challenges associated with effectively utilizing pyrometry in RTP have prompted investigation into a number of alternative methods.

The traditional alternative to a pyrometer has been the thermocouple. A thermocouple is a pair of contact probes made out of different materials. When the two ends of the probes are placed in contact with a material, a change in its temperature creates a voltage. The voltage can then be used to determine the temperature of the material.

The impracticality of employing this type of a contact-based measurement method in an RTP system is, however, fairly apparent. Besides potentially contaminating the wafer with foreign substances, surface contact is also insufficient for obtaining absolutely accurate measurements. These would require the thermocouple to be welded to the wafer's surface, which adds a highly impractical preparation step into the process. For this reason, thermocouples are only used for highly specific applications and for the cross-calibration of pyrometers [35, 36]

Another method is fiber optic thermometry, which utilizes an optical sensor head at the end of a fiber optic cable. This can be used in combination of a pyrometer to place the sensor head very close to the measured material, thus lessening the effects of stray radiation on the readings [39]. The probe's exposure to heat in the chamber may, however, pose a problem in some RTP systems.

A variant of this method, which is not based on pyrometry, is the fluoroptic thermometer, which instead of an optical sensor head has a probe tip containing phosphorus. When exposed to heat, the phosphorus produces a fluorescent glow. The intensity of the effect depends on the temperature; hence temperature can be determined by measuring the duration of the afterglow. This requires contact with the wafer, but the method is non-destructive, unlike thermocouple attachment, and the sensor tip can potentially be coated with an inert material to minimize contamination [40].

Another method, developed specifically for RTP, is acoustic thermometry. The method is based on utilizing the wafer holding pins to transmit and receive vibration. One of the pins is connected to an actuator which causes the pin to vibrate at a specific frequency. The vibration is transmitted through the wafer to another pin, which is connected to a sensor. As the frequency of the vibration changes based on the temperature of the medium, the wafer's temperature can be determined by comparing the frequency of the received vibration to that of the source [37].

2.3.4 Control

A basic method of controlling wafer temperature employed in many RTP systems is a closed loop system based on feedback from the temperature sensors. The measured value is compared to a temperature setpoint in the control software, which typically employs a PID control scheme. A control signal is then fed to the power controller which supplies power to the system's heat source [32].

A large number of more advanced control schemes have been developed to address problems such as inaccurate temperature measurement and wafer temperature disuniformity. These often include complex mathematical modeling of the radiation physics inside the RTP chamber [41 – 43].

Since advanced control science is outside of the author's field and competence area, these will not be covered in more detail in this thesis.

3 Heater design

The physical structure, instrumentation and control scheme of the existing heating module design are detailed in this chapter. Additionally, the overall operation of the cluster tool is summarily explained in order to present a comprehensive picture of the heater's role and purpose.

The heating station constitutes one part of a larger wafer loading system, which together with an ALD reactor forms a cluster tool. Central to the loading system is a large vacuum chamber, referred to as a *transfer module*, containing a SCARA type wafer handling robot. The cluster's process modules are attached to this central chamber. During wafer processing, individual wafers are cycled through the process modules in a pre-specified sequence before they are loaded into the ALD reaction chamber. In the ALD reactor itself, the wafers are processed as a batch, arranged in spaced slots within a holding rack. Wafers enter the system through an infeed port, which may be connected to either an operator-loaded airlock or a buffer station connected in turn to another wafer handling system.

The layout of a typical wafer loading system used by Beneq, ALD reactor excluded, is depicted in figure 12.

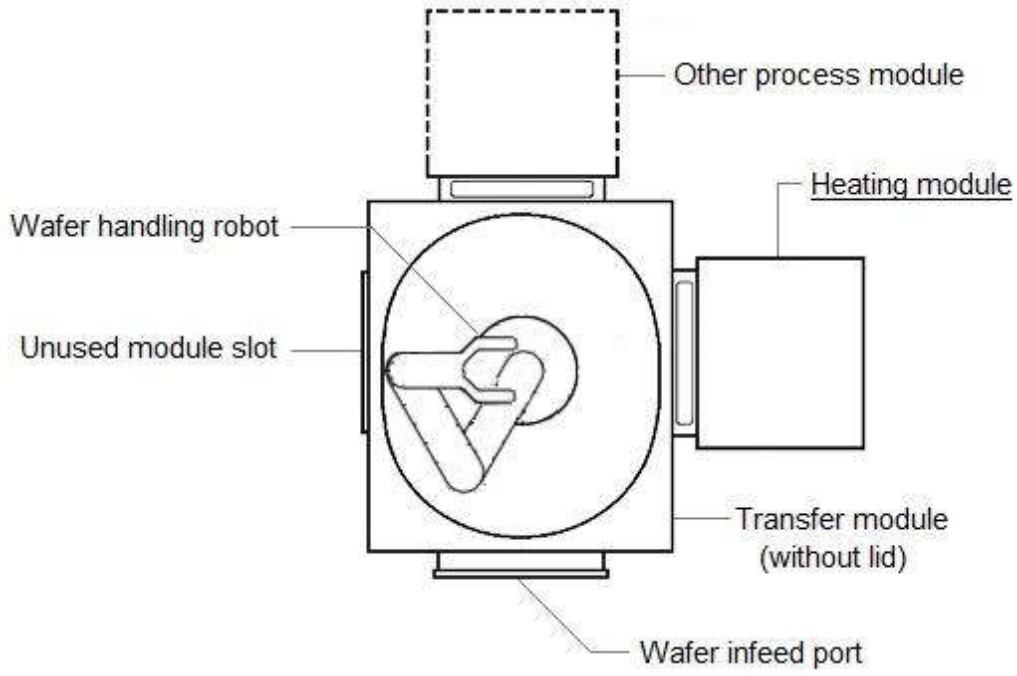

Figure 12. Simplified schematic representation of the wafer loading system, indicating the placement of the heating module. The figure depicts the loader from above.

The heating station is used for the rapid pre-heating of wafers prior to their insertion into the ALD reaction chamber. This is done to circumvent the warm-up phase that would otherwise be necessary to bring the wafers to the target process temperature inside the reactor. As the reactor is heated using resistive elements and the processing is done under vacuum, heating large lots of wafers in this manner can take up to an hour due to the poor heat transfer rate.

The importance of the pre-heating step is emphasized particularly in the growing of thinner coatings, since the processing times required to grow these are shorter. The shorter the processing times are, the more undesirable a long warm-up period becomes.

Rapid thermal processing of the wafers inside the reaction chamber itself is not possible due to various restrictions imposed by the reactor's physical design. In addition, the wafers' arrangement one on top of the other in the reactor's holding rack results in the topmost wafers of the stack acting as a heat shield, which renders the batch processing approach ineffective for heating. A separate, single-wafer heating module is hence required.

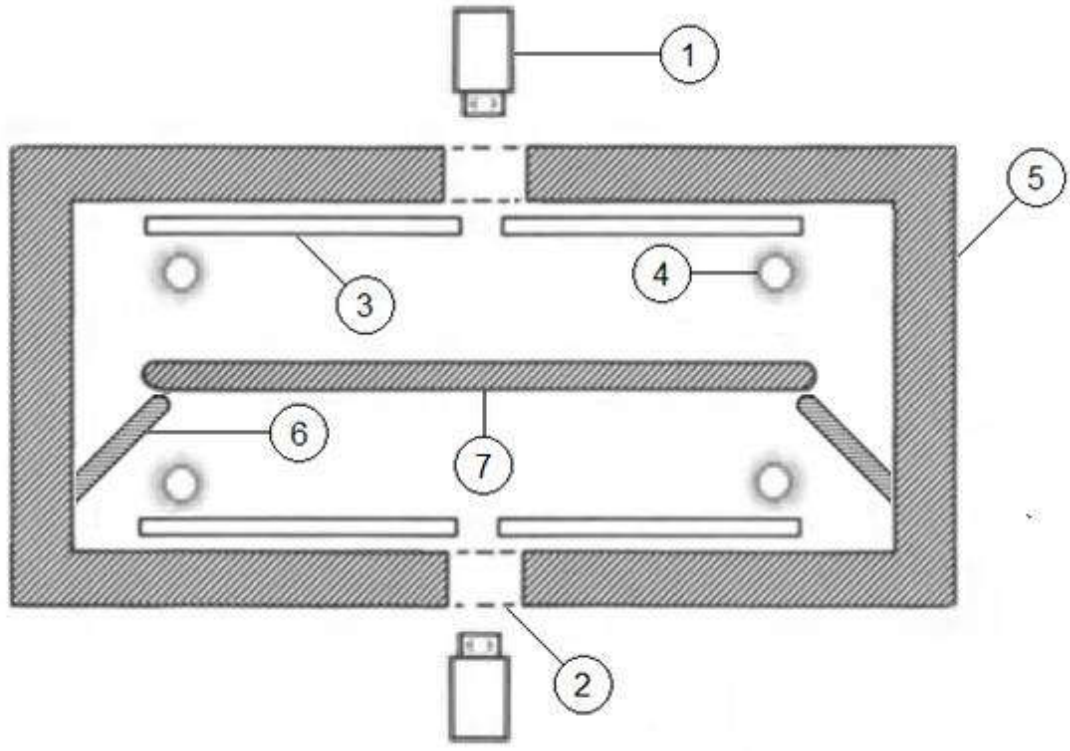

Figure 13. Schematic diagram of the heating module. The labels indicate the following parts: (1) Pyrometer, (2) IR-permeable window, (3) Reflector plate, (4) Ring-shaped IR lamp, (5) Metal chamber wall, (6) Wafer holding pin, (7) Wafer.

The heating module design consists of a horizontally symmetrical aluminium vacuum chamber housing a high-power radiant energy source. Inside the chamber, the wafer is suspended on holding pins with the contact points tapered in order to minimize the contact area. Wafers are moved in and out of the chamber through an opening by the robot positioned in the adjacent transfer module. The chamber opening does not have a gate valve, and as such, the heating chamber always shares environmental conditions with the transfer module.

Outside of maintenance and troubleshooting, the chamber is kept under vacuum. The degree of vacuum ranges from medium (3 kPa – 0.1 Pa) to ultra high (0.1 µPa – 0.1 nPa [44]) depending on the customer's specifications.

Wafers are heated from both sides using two short-wave infrared emitters. A single emitter consists of a tungsten filament inside a ring-shaped quartz tube, the ring being roughly of the same diameter as the heated substrate. The backside of the tube is dimmed using a reflective coating that ensures that all emitted radiation is directed at the substrate. Additionally, between the emitter and chamber wall there is a polished aluminium reflector plate which serves the same purpose.

Since the specific ALD processes for which the tool is designed for are in the low temperature range (100-200 °C), the heating chamber does not incorporate an active cooling feature.

Wafer temperature is measured from the wafer's center using two pyrometers positioned at the opposite sides of the chamber. As the pyrometers are not designed to withstand vacuum or direct heat exposure, they are installed outside of the chamber and view the substrate through special IR-permeable windows.

The spectral range of the pyrometers is 8–14 µm, which is a region commonly used in pyrometry and thermal imaging for generic applications [45]. The temperature measurement range encompasses the full range from an ambient (room) temperature to a peak process temperature. Additionally, the pyrometers are equipped with close-focus optics which narrow the measuring area to a diameter of a few millimeters at the measuring distance used in this design.

The structure of the heating chamber and the positioning of the heater's instrumentation are depicted in figure 13.

Power is supplied to the IR emitters through a relay. The power control of the emitters is essentially an on/off action; the wattage supplied to the emitters is always constant. Scalar power control is instead achieved using a method called time proportioning, in which the cycle time is portioned to alternating on and off periods. The relative lengths of these periods are based on the desired level of power output. Over multiple consecutive cycles, this results in the average emitted energy to be at the desired level. For example, if the desired energy output is 60% of the maximum, the heaters would be turned on for a duration of 60% of the employed cycle time. This example is demonstrated in figure 14.

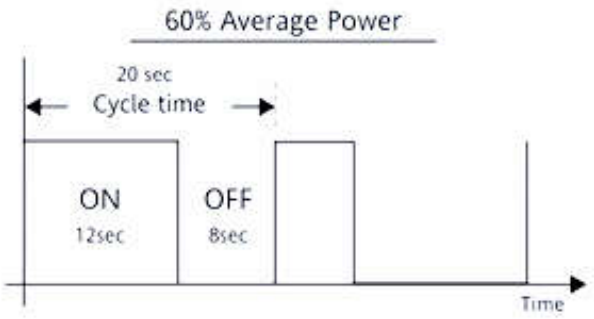

Figure 14. Example of a time-proportioned cycle [46].

Overall process control is in turn accomplished using closed-loop feedback from the pyrometers. The target temperature for the heating is set through the tool's control software. Once the temperature reading of the two pyrometers reaches the target temperature, the heating is turned off.

In summary, wafers are placed sequentially into the heating module, where they are heated using short-wave infrared radiation while the chamber is under vacuum. Wafer temperature is measured in a contact-free manner using pyrometry. The temperature readings are referenced against a user-defined setpoint, and heating is disengaged when the setpoint is reached. The wafers are then moved into the main process chamber, in which they are processed as a batch after the entire lot has been loaded in.

The significance of some design features detailed in this chapter in terms of the heater's operation is discussed further in the following chapters.

4 Investigation & analysis

This chapter details the investigation into the heating module's function and the analysis of the observations based on the theory covered in chapter 2.

It should be noted that although the theory section of this thesis is covered in an earlier chapter, the chapter arrangement does not represent the chronological progression of the work. At the time of some the tests covered in this chapter, parts of the theory covered earlier were unknown to the author and were only investigated afterwards to explain some of the results of the tests. Some of the findings of the literature survey will hence be repeated in this chapter when they are relevant for analyzing the results.

4.1 Tools and equipment

Tests were conducted with two separate wafer loading systems, the first of which was designed to handle 200 mm wafers, while the second was designed for 300 mm wafers.

The wafer loading systems belonged to tools undergoing final testing at Beneq's facilities prior to their shipment to customers. The fact that the tests were conducted with customer projects rather than a pilot tool dedicated for product development purposes placed a number of constraints on the testing process. All tests had to be fitted within a fairly strict testing and commissioning schedule and were limited by the tools' specifications (for example, temperature limits for the heating). Furthermore, the tests could not be too intrusive and no significant modifications could be made to the tools to accommodate testing.

A limited selection of instrumentation and other testing equipment was available in-house. These included:

- The pyrometers included in the heating station's design, operating in the spectral range of 8 – 14 µm.
- A handheld thermographic camera likewise operating in the 8 – 14 µm band. The camera had an aperture with a diameter of 35 mm and a measurement range of -20 – 350 °C.
- Silicon and glass wafers for testing, in sizes of 200 and 300 mm for silicon and 200 mm for glass.

Equipment specifically requisitioned for the testing included:

- An additional pyrometer using the 8 – 14 µm band. This was equipped with an USB connector, which allowed it to be connected to a PC for temperature monitoring.
- Another pyrometer with a spectral range of 2 – 2.6 µm, likewise equipped with an USB connector.
- A zinc selenide window inside a vacuum flange assembly. This was used to take pyrometric and thermographic measurements from inside the vacuum transfer module. ZnSe was chosen because the material has a very wide transmission band (0.6 – 16 µm) [33] in the IR spectrum, making it permeable to most IR wavelengths. The view diameter of the widow was 34 mm, which corresponded closely with the thermal camera's aperture size.

Employing a contact-based measurement method such as a thermocouple or an adhesive temperature label for the verification of wafer temperatures was considered, but these could not be acquired in sufficient time for the tests.

4.2 Serial heating tests

The first series of tests were conducted with the 200 mm wafer handling system. A wafer cassette containing 15 wafers was inserted into the loader and an automatic loading sequence containing the pre-heating step was commenced, so that the wafers would be successively cycled through the heating station. The temperature setpoint for the pre-heating was 60 °C**.** The same test was conducted once using a batch of glass wafers and again using silicon wafers. The heater was allowed to cool to ambient temperature between the tests.

The temperature of the wafers was measured simultaneously using two different measuring instruments: a pyrometer and the thermographic camera. The pyrometer on the top side of the heating chamber was removed and its viewport used to measure the wafer using the thermographic camera described earlier. Temperature readings were then logged simultaneously from the bottom pyrometer (which was left in place) and the thermal camera. The purpose of this was to test the heater's function while independently verifying the temperature readings using an instrument not connected to the system.

Table 1. Thermal camera readings for glass, in °C.

1	27,8	25,9	45,5
2	150 >	29,9	54,6
3	150 >	32,2	56,3
4	150 >	33,6	55,6
5	150 >	34	58,7
6	150 >	35,2	57,4
7	150 >	36,6	57,4
8	150 >	35,7	57,8
9	150 >	37,6	58,3
10	150 >	37,9	59
11	150 >	39	588
12	150 >	40	58,6
13	150 >	39,3	58,5
14	150 >	39,9	60,4
15	150 >	40,1	60,3

Table 2. Pyrometer readings for glass, in °C.

1	27,3	28,1	62
2	105	34,2	60,1
3	115	37,5	64
4	119	39,8	62,1
5	126,7	42,6	62,3
6	129,7	41,9	63,5
7	132,2	40,6	62,3
8	135,6	41,2	62,7
9	139,5	44,2	65,3
10	140,7	43,7	68,2
11	142,3	45,1	69,6
12	142,7	45,8	65,1
13	141,7	43,6	70,1
14	144,3	44,9	69,2
15	144,5	43,6	69,4

Substrate temperature after heating

Substrate temperature before heating

Chamber temperature

Table 3. Thermal camera readings for silicon, in °C.

1	28,2	28,4	56,8
2	58,7	47,7	65,6
3	75,3	49,5	61,6
4	71,6	46,8	69,6
5	77,6	55,8	71,6
6	107	51,3	64,5
7	106	56,9	69,6
8	117	57,8	57,8
9	130	54,2	66,4
10	124	60	81
11	119	62,8	62,8
12	124	59,4	72,4
13	136	61,3	61,3
14	128	57	76
15	134	55,6	55,6

Table 4. Pyrometer readings for silicon, in °C.

1	29	29	64,3
2	64,2	47,7	67,2
3	68,3	56,2	68,7
4	74,3	52,4	65,2
5	73,1	56,6	63,4
6	72,4	56,6	62,1
7	75,1	55,6	69,9
8	74,4	61,7	61,7
9	72,8	54,7	67,1
10	75,1	56,9	69,6
11	68,1	60,7	60,7
12	72,9	56,7	67,2
13	72,9	62,1	62,1
14	72,7	54,7	68,4
15	73	60,7	60,7

A number of methodological errors with the measurements necessitated repeating the tests several times. The data from two tests where the initial conditions were identical and the testing was conducted using the same methods is presented in tables 1 – 4. Tables 1 and 2 present the data from the first test, conducted with glass wafers, while 3 and 4 list the results from the second, in which silicon wafers were used.

As explained by the annotations under table 1, the second column lists the temperature reading from the empty chamber (i.e. the polished aluminium reflector plate on the opposite side of the chamber) prior to the insertion of the wafer. The second column lists the temperature reading acquired from the wafer after it has been placed inside the chamber but before the IR emitters were turned on. Finally, the third column gives the wafer's temperature readings immediately after the emitters had disengaged.

The red highlighting in tables 3 and 4 indicates that the IR emitters did not turn on at all.

The chamber temperature in the first table is listed as 150 > because the thermal camera was unable to read temperatures of over 150 °C. It was initially unclear why this would be the case despite the high end of the camera's measurement range being given as 350 °C.

As the emissivity settings used for the measurements were set to correspond with the emissivity of the measured substrates, the temperature readings taken from the empty chamber are likely not entirely accurate. However, a clear trend of gradual heating of the chamber corresponding to the number of consecutive heating instances can be observed from the data. Measurements taken from other points in the chamber's interior using the thermographic camera also confirmed that the rise of temperature was significant across the interior surface of the entire chamber and not only the reflector plate.

Another trend clearly observable from the data is the gradual increase of the initial wafer temperature readings tied to the number of consecutive heating instances. The effect is less pronounced for glass but quickly becomes problematic in the case of silicon. As can be seen from tables 3 and 4, the initial temperature reading reaches the setpoint value already after the 7th heating, after which the IR lamps begin to fail to engage for every second wafer or so.

While heating times were not logged during the tests and are therefore missing from the tables, a gradual shortening of heating times was observed during the tests. This was particularly the case with silicon wafers. While after the 8th heating the emitters did engage in some instances, the temperature differential between the initial reading and the setpoint was so small that heating times for the latter part of the batch were very short, ranging from less than a second to a few (usually no more than three) seconds.

It was clear from the results that the problem had to do with the chamber structures retaining a portion of the thermal energy generated by the IR lamps during heating. It was not clear if the elevation of wafer temperatures was entirely a result of the distorting effects of background radiation on the pyrometers or if there was heat transfer taking place between the wafer and the chamber walls.

Another issue to contend with was the high reflectivity of silicon wafers. The issue is well illustrated by the thermographic profiles of the two types of wafers shown in figures 15 and 16. These were acquired by using the thermal camera to view the wafers through the pyrometer viewport on the top side of the heating station. Both of the images are of heated wafers, and were taken after the IR lamps had disengaged.

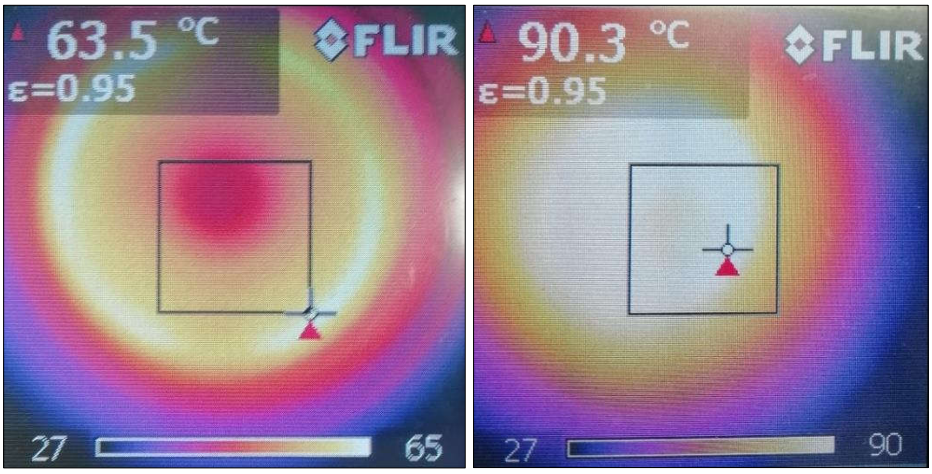

Figures 15 and 16. Thermographic profiles for a silicon (left) and a glass (right) wafer.

As can be seen from the image, much more variation in temperature can be seen on the silicon wafer's surface. While this could be initially mistaken for a real heat gradient, it seems to actually be a result of reflections of the chamber surroundings. The bright ring visible at the silicon wafer's edge is most likely a reflection of the IR emitter's quartz tube,

while the dimmer spot at the wafer's centre is the viewport through which the wafer is being imaged. The glass wafer does not exhibit the same effect due to its lower reflectivity.

The high reflectivity of the silicon wafers could also be the reason why the thermal camera's readings peaked at 150 °C: the camera's readings were distorted by radiation reflecting from the wafer's surface which had a wavelength distribution partially or entirely outside the camera's spectral range.

4.3 Heat transfer in vacuum

While analyzing the results of the previous series of tests, it became clear that it was necessary to be able to measure wafer temperature outside of the heating station, where measurements would not be affected by the background radiation and reflection effects present inside the chamber.

This was initially not possible due to the viewports on the transfer module's lid being borosilicate, which is not IR-permeable. Removing the wafer from the wafer handling system for imaging was not a workable solution as in the process of venting the system, the wafer would be exposed to room temperature air and cool down as a result.

To allow for measurements to be taken from inside the transfer module while it was in vacuum, an IR viewport (the ZnSe window described at the beginning of the chapter) was installed on the transfer module lid. This was done by removing one of the borosilicate windows and replacing it with the ZnSe viewport. Since the ZnSe window was of a smaller diameter than the borosilicate one, it was fitted into an aluminium plate with the same diameter as the silicate window. The assembly is pictured in figure 18. Its place of installation in the transfer module is indicated in figure 17.

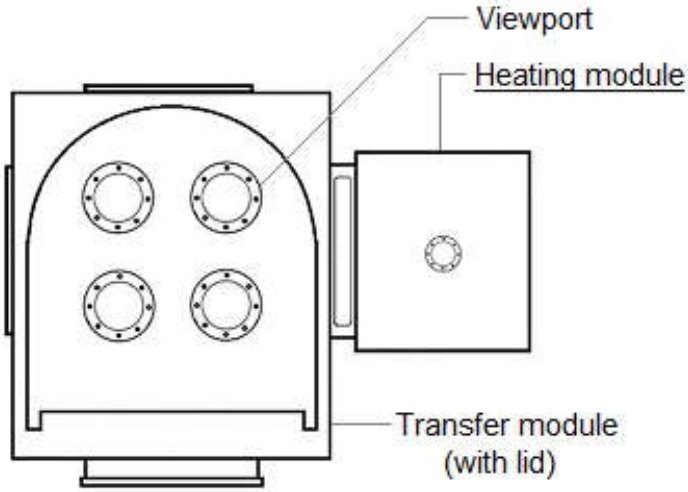

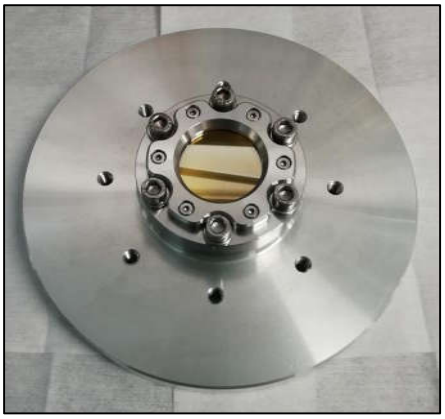

Figures 17 and 18. The zinc selenide viewport assembly (right) and its positioning in the transfer module (left).

A measurement position outside of the heating station allowed wafers to be removed from the station and measured in a space where the surroundings were at ambient temperature.

The first tests were done to determine if there was a significant degree of heat transfer occurring between the hot inner chamber wall and the wafer by means of radiation.

This was done by heating an empty chamber until the pyrometers reported the chamber temperature as approximately 150 °C, which was the highest temperature recorded during the serial heating tests. A silicon wafer at ambient temperature was then inserted into the chamber, kept inside for various lengths of time (approx. 3, 10 and 15 s.), and then withdrawn to be measured outside of the heating chamber.

Measurements performed using the instrument positioned outside of the heater showed no appreciable increase in wafer temperature regardless of the time the wafer was kept inside the heater. The pyrometers measuring the insides of the chamber continued to show a reading significantly higher than ambient, as in the previous heating tests.

This supports the intuitive notion that aluminium at the comparatively low temperature of 150 °C does not radiate strongly enough to transfer any significant amount of energy to the wafer. Convection, in turn, cannot occur in vacuum, and conduction is limited due to the wafer holding pins and the wafer having a very small contact area.

It was thus determined that the initial wafer temperature being displayed as higher than ambient is wholly the result of the distorting effects of background radiation on pyrometric measurements.

The question of the rate of heat transfer by radiation in vacuum brought forward the idea of additionally testing the rate by which silicon wafers cool while in vacuum. This was mostly done in order to determine how much the wafer should be expected to cool during its transfer from the heating station into the processing chamber.

A prediction for maximum cooling rate of a silicon wafer found in the source literature is presented in figure 19. The prediction assumes ideal conditions, in which the wafer is located in a fully black enclosure which is in room temperature [47]. As can be seen from the figure, the rate of cooling is dependent on the wafer's temperature, with higher temperature corresponding with a faster cooling rate.

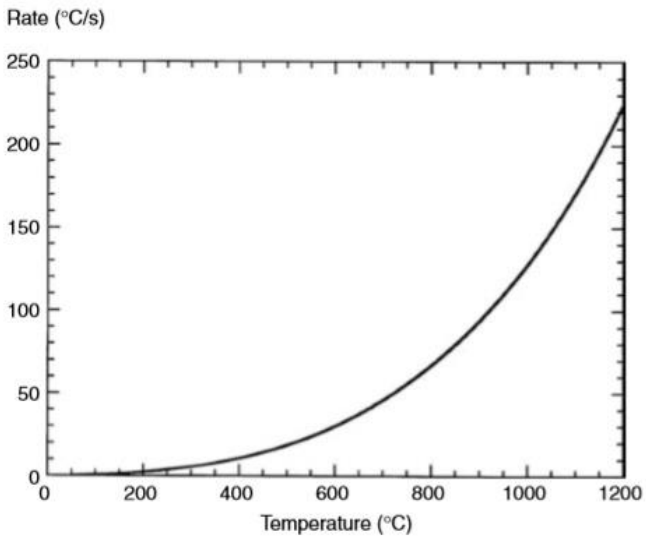

Figure 19. Prediction of the cooling rate of silicon wafer across a temperature scale [47].

To record the rate of cooling across a sufficiently wide temperature scale, a wafer was heated to approximately 250 °C and brought to the measuring point outside of the heater. Figure 20 shows the temperature graph recorded by the pyrometer between temperatures of approximately 250 and 150 °C.

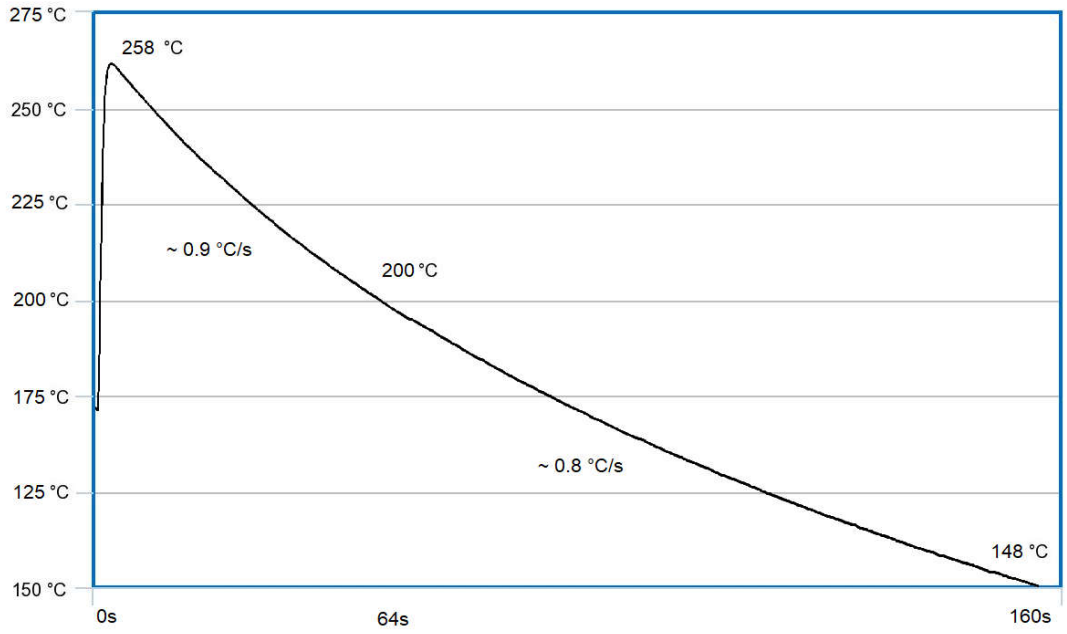

Figure 20. A wafer's temperature as a function of time as the wafer cools while in vacuum.

As can be seen from the figure, in real-life conditions the cooling rate is somewhat lower than in ideal conditions. Starting from 250 °C, the rate is ~0.9 °C/s, which is less than half of the approximately 2.5 °C/s predicted for this temperature. The cooling rate does, however, decrease proportionally to the temperature as predicted by the model. At 150 °C it has decreased to around 0.7 – 0.8 °C/s, and at 100 °C (not pictured) it is as low as 0.3 – 0.4 °C/s.

Additionally, an attempt was made to image a wafer using a thermal camera positioned at the viewport in the transfer module lid. The intent was to determine how much the temperature differed at the center of the wafer and at its edges. However, as in the thermal images acquired from wafers inside the heater, reflections of the surroundings on the wafers surface occluded the wafer's thermal profile, making it extremely difficult to discern a heat gradient.

4.4 Effects of wavelength selection

To test the effects that the pyrometer's wavelength selection has on the reliability of the measurements, one of the heating station's pyrometers was replaced with a pyrometer operating in the short wavelength range. As explained at the beginning of this chapter, the

full theory behind the pyrometric measurement of silicon was not known at the start of these tests. The spectral band of the pyrometer was instead chosen based on a number of non-scientific sources such as product brochures [48, 49], which generally recommend shorter wavelengths for measuring reflective surfaces at lower temperatures.

Hence a pyrometer with a spectral range of 2 – 2.6 µm was chosen for testing with the expectation that it would be less prone to measurement errors than the 8 – 14 µm pyrometer used in the existing heater design.

It quickly became apparent, however, that this was not the case. The pyrometer showed a dramatic leap (over 600 °C) in its temperature readings when the lamps were powered. It was suspected that this was due to the pyrometer detecting the lamps' radiation. A consultation of literature on the subject confirmed this suspicion: while the datasheet for the IR emitter reported the lamp's "peak wavelength" as 1 – 1.4 µm, a graph found in one publication (shown in figure 21) demonstrates that the spectral distribution of the radiation emitted by a quartz-enclosed tungsten-halogen lamp has significant overlap with the pyrometer's spectral range.

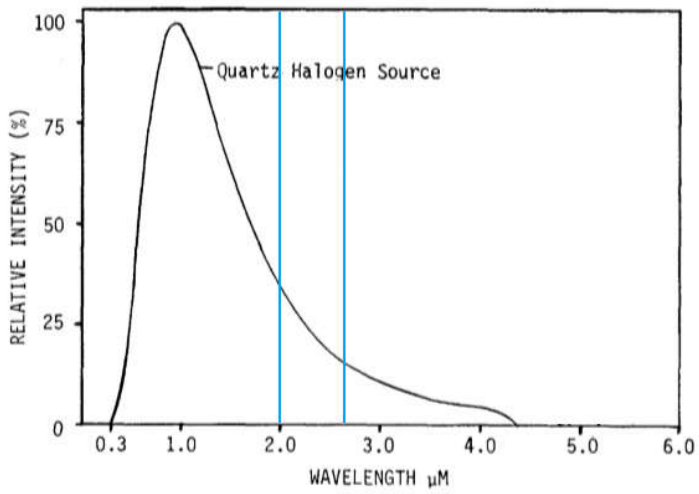

Figure 21. The wavelength distribution of a quartz halogen radiant source.

Another anomaly observed during the tests was that the temperature reading did not seem to change when the wafer was removed from the chamber. Investigating further, the pyrometer did not report a significant change in the reading when a wafer was inserted into the heater either. This was true for both wafers at ambient temperature and ones that had been heated and then removed from the heater. The pyrometer only reported an

appreciable change in temperature when the robot's end effector passed directly underneath it while transporting a wafer into or out of the heater.

These observations seem to indicate that the wafer is completely transparent to the pyrometer. This interpretation is supported by the source literature: figure 22 shows the emissivity of silicon at various temperatures with the spectral bands of the two kinds of pyrometers tested marked on the graph.

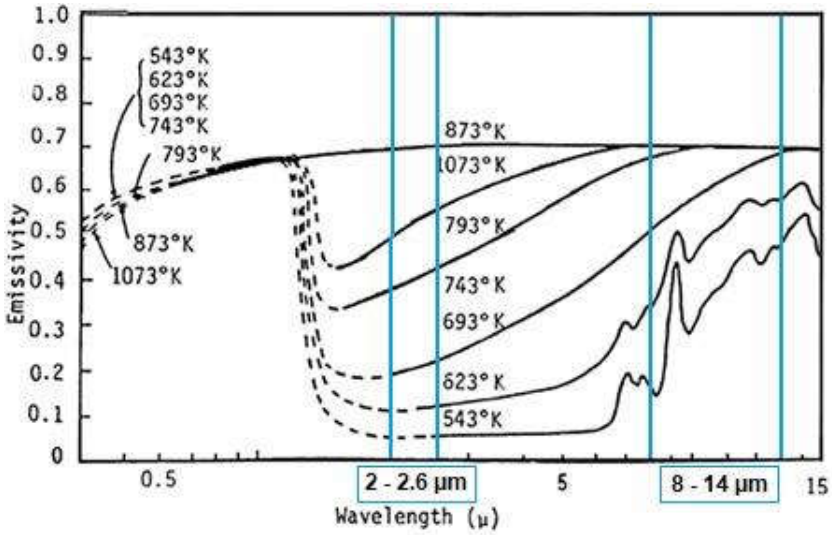

Figure 22. A graph showing the spectral emissivity of silicon in different temperatures, with the spectral bands of the two pyrometers marked on the wavelength scale.

As can be seen from the figure, at temperatures of and under 543 K (270 °C), silicon exhibits almost no emissivity at the 2 – 2.6 µm wavelength range. In the 8 – 14 µm range, however, it is somewhat emissive even at lower temperatures. Low emissivity means high transmission, which explains why the long-wave pyrometer was able to "see" the wafers while the short-wave one was not.

4.5 Effects of emissivity settings

Since the source literature states that chamber geometry and reflectivity can affect the effective emissivity of a silicon wafer, a series of tests were conducted to determine the degree by how much temperature measurements were affected by the pyrometer's emissivity setting.

In the tests, a wafer was heated to a target temperature of 100 °C using three different emissivity settings for the heater's pyrometer. The wafer was then removed from the heater and measured again outside of the heating station using the same three emissivity settings. The IR viewport installed on the transfer module lid was used again to provide an outside measurement position.

The emissivity settings used were:

- ε = 1, the maximum possible value
- ε = 0.7, silicon's constant emissivity value at higher temperatures
- ε = 0.4, the average emissivity of silicon in the 8 – 14 µm range at lower temperatures

The most illustrative of the expected effect was the test made with the heater's pyrometer set to ε = 1. The emissivity of the second pyrometer was initially 1, which was adjusted to 0.7 and again to 0.4 The resulting graph is shown in figure 23.

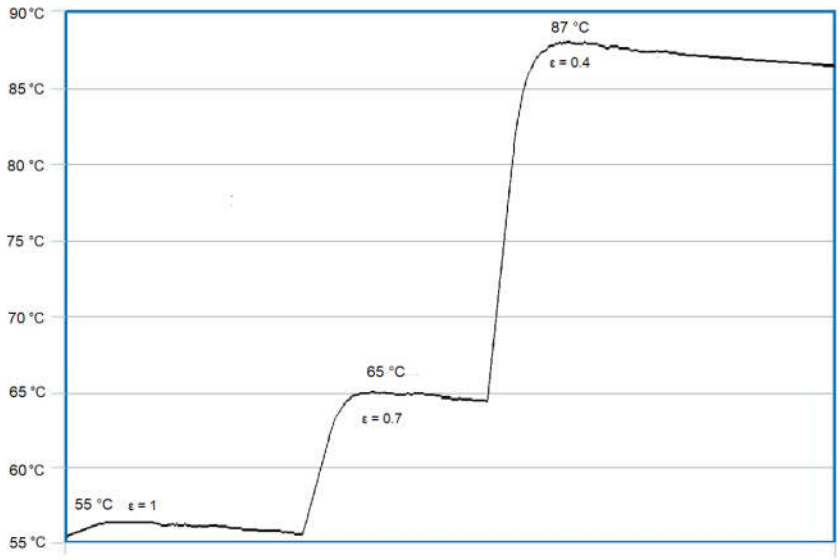

Figure 23. Temperature readings of the second pyrometer using three different emissivity settings.

The graph demonstrates clearly that the emissivity setting of the pyrometer positioned outside of the heater had to be adjusted to a value significantly lower than that of the pyrometer in the heater to obtain comparable results.

In this case, the temperature reading obtained using an emissivity value of 0.4 is likely closest to the truth, as this is approximately the average emissivity of silicon at temperatures lower than 270 °C [34], and the measurements were done away from the distorting effects of the heated chamber.

However, using an emissivity value of less than 1 for the heater's pyrometer resulted in shorter heating times, and consequently lower actual temperatures, all the while the pyrometer reported the wafer temperature as equal to the target value.

In short, it was necessary to significantly overestimate the wafer's emissivity in order to heat the wafer to the desired temperatures.

4.6 Miscellaneous observations

It became apparent during the serial heating tests that the heater's control scheme was not functioning as intended. Inquiry into the issue revealed that this was due to the time-proportioning scheme's (detailed in chapter 2) proportional term having been set to a value that effectively negated the time-proportioning and turned the heater's control into an on-off action. This was a carryover from a previous customer project, and was apparently done due to concerns about the durability of the heater's electromechanical relay under constant rapid switching as well as the control scheme's effect on overall heating time.

Furthermore, it was observed that time required to heat 300 mm wafers to some of the target temperatures used in the tests was slower than desired. It typically took 30 s to heat a 300 mm wafer to temperatures over 100 °C, and close to two minutes for higher temperatures such as the 250 °C used in one of the tests. This seems to be a result of the heaters originally having been sized for 200 mm wafers, and 300 mm wafers having more than double the mass and surface area.

5 Design revision

With the problems affecting the heating station identified, and several examples of sufficiently similar constructions having been found in the body of publications on the subject, a revision of the design can be attempted.

The design changes proposed in this chapter are made under the confines of a number of limitations. The foremost of these was a fairly restrictive project schedule, which discouraged making radical changes to the initial design. The least amount of changes necessary to achieve the intended improvement in functionality were hence made. Additionally, since the heater was a part of a larger cluster tool design marketed as a product, the manufacturing costs and the costs of the module's instrumentation were to be kept at a reasonable level. This ruled out the implementation of some of the more novel solutions covered in the theory section. These considerations dictated for the basic concept of heating by incoherent infrared light coupled with pyrometric temperature measurement to be retained.

Some key differences between the purpose and application of the heater design and the RTP systems presented in the source literature should be noted. These are:

- No chemical processes are conducted inside the chamber concurrent with the heating. This removes the need to isolate the wafer atmospherically from the rest of the chamber, e.g. by a quartz gas seal used in RTPCVD applications shown in chapter 2.3.2.
- Wafers are heated to relatively low temperatures compared to some of the designs found in the source material. In systems designed for high temperature (> 600 °C) processes, silicon can be treated as an opaque material. In this design, the process temperatures are low enough to necessitate taking silicon's partial transparency in the IR spectrum into account.
- After heating, the wafers are moved into a process chamber which is kept at a constant temperature, where they remain for some time (several minutes at the minimum) before ALD processing begins. Temperature uniformity control does not therefore need to be as stringent as in typical RTP designs and there is more tolerance for deviations from the temperature setpoint. This means that design features with the primary function of improving temperature uniformity, such as wafer guard rings, are largely unnecessary.

5.1 Physical design

It seems clear, based on the results of the serial heating tests as well as examples of functional thermal processor designs presented in the source literature, that the primary problem with the existing chamber design is the lack of an active cooling feature. This causes the chamber's interior walls to heat up as a result of consecutive heating instances, turning them into a source of background radiation which distorts pyrometric measurements.

Following he recommendation given by the source literature for chamber designs of this type, the chamber should have water cooling channels inside its walls.

Besides active cooling, another way of reducing background radiation inside the chamber is to polish the chamber walls. This has the effect of increasing reflectance at the expense of emissivity. The effect that surface roughness has on the emissivity of aluminium is demonstrated in figure 14. Highly reflective chamber walls are preferable to highly emissive ones since reflected radiation retains its characteristic wavelength. As the spectral ranges of the IR emitters and pyrometers do not overlap, the reflected radiation is not detected by the pyrometers and hence does not disturb measurements. In contrast, thermal energy absorbed by a highly emissive surface will be at least partially radiated out at wavelengths characteristic to the material of the surface, which the pyrometers may be sensitive to. The wavelengths at which aluminium is emissive can likewise be seen from figure 24.

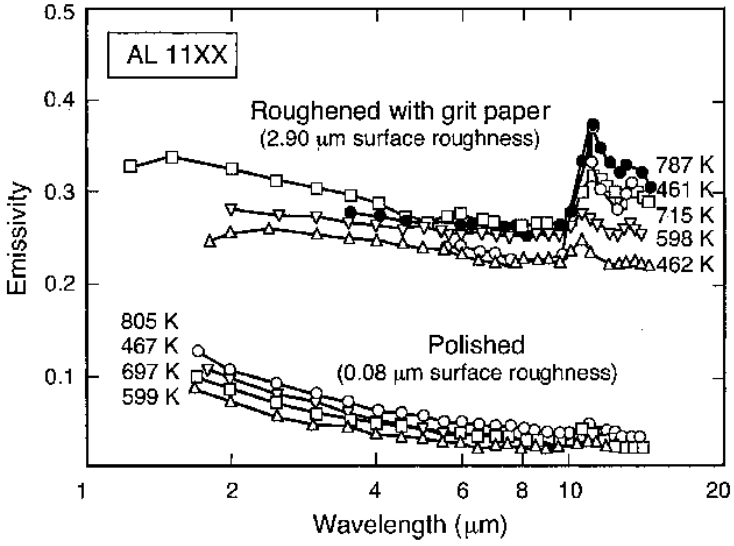

Figure 24. Emissivity of an aluminium alloy at different temperatures [50]

The polishing method used for similar chamber designs in the source literature is electropolishing, or alternatively coating with a reflective material. A more cost-effective solution would be to cover the chamber walls entirely with reflector plates. These would have to have contact points with the water-cooled chamber walls to conduct away heat as well as have as little mass as possible to minimize heat retention. Ideally, the reflector plates should be polished aluminium. Gold and silver, though highly reflective, are to be avoided due to the risk of metal contamination [51].

Yet another source of unwanted background radiation are the quartz envelopes of the IR emitters themselves. The quartz tube can heat up to temperatures of up to 400 °C, which turns it into a secondary radiation source that remains active even when the lamps are unpowered. Since the surface of the quartz tubes cannot be altered without affecting the function of the lamps, the problem must be addressed with pyrometer wavelength selection. This will be discussed later in this chapter.

Otherwise, the ring-shaped tungsten-halogen IR emitters present in the existing design are a fairly sound choice for a heat source and should be retained as-is. Out of specifically radiant heat sources, a short-wave emitter such as this is in fact the best choice due to silicon turning transparent in the middle-infrared range. While the heating rate for particularly 300 mm wafers was observed to be less than desired, replacing the heat source with a more high-power lamp configuration - such as the honeycomb array or the cross-grid design shown in chapter 2.3.1 - would require a radical redesign of the chamber housing.

The power output of the heat source can be increased instead by adding a second and possibly a third lamp of a smaller and/or larger diameter to create an array of concentric lamps on each side of the chamber. Spiral-shaped lamps are also available from the same manufacturer; however, multiple individual lamps may be a better option since this enables to control the power output of each of the lamps individually. This would make it possible, for instance, to compensate for the heat loss at the wafer's edges by supplying relatively more power to the outermost lamp in the array.

The pyrometer's wavelength selection is of particularly crucial importance. The wavelength range between approximately 1.5 µm and 6.5 µm is not usable due to silicon's near-total transparency at these wavelengths in temperatures below 600 °C (see figure 25). Wavelengths below 1.5 µm must also be disregarded due to the IR lamps outputting radiation in

the short-wave range. The 8 – 14 µm range used by the pyrometers in the current design falls within the remaining area but is inoptimal due to the width of the spectral band and the high degree of emissivity variation exhibited by silicon within it.

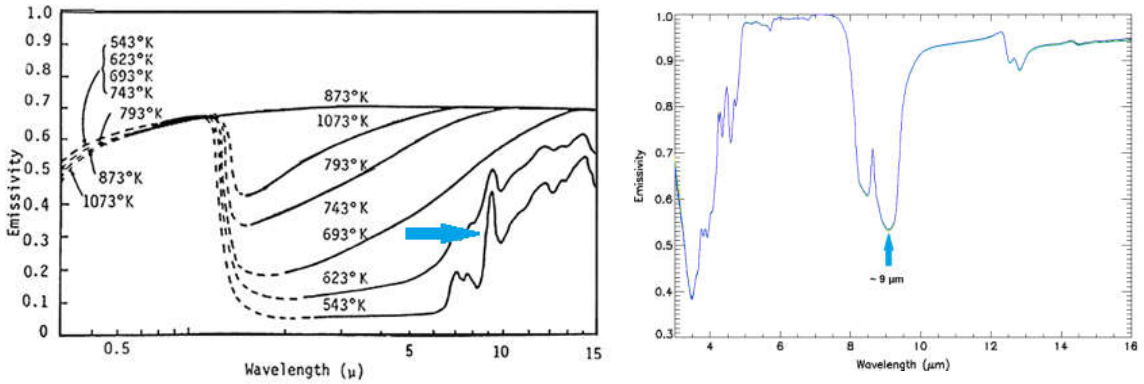

Figures 25 and 26. Spectral emissivity of silicon, showing a spike at roughly 9 µm (left). Spectral emissivity of quartz, showing a dip between 8 and 9 µm (right) [52].

The most ideal solution would be to use a single wavelength or a very narrow wavelength range which falls inside the limits of 6.5 µm and 15 µm. This would allow the wafer's emissivity value to be known exactly, as well as its change in response an increase in wafer temperature to be predicted more reliably.

An examination of the emissivity graphs of silicon and quartz (figures 25 and 26, respectively) shows that silicon exhibits an upward spike in emissivity at approximately 9 µm, while quartz exhibits a drop in emissivity within the range between 8 and 9 µm. A pyrometer operating at this spectral range would hence be the least sensitive to radiation emitted by the IR lamps' quartz casing while remaining sufficiently sensitive to the radiation emitted by the wafers.

While single-wavelength pyrometers exist, there is a limited selection of wavelengths used by off-the-shelf instruments available on the market. These do not include any wavelengths between or sufficiently close to 8 and 9 µm. Custom solutions may be available, but these can be expected to be unreasonably expensive for their application.

An alternative solution would be to use a standard 8 – 12 µm or 8 – 14 µm pyrometer and use an optical material to filter out the longer wavelengths. By chance, a material suitable for this exists: calcium fluoride, as depicted by figure 27, is fully transparent until 8 µm, after which it becomes gradually less transmissive. A pyrometer with its measuring range starting from 8 µm coupled with a calcium fluoride window would be sensitive mostly to wavelengths between 8 ~ 9.5 µm.

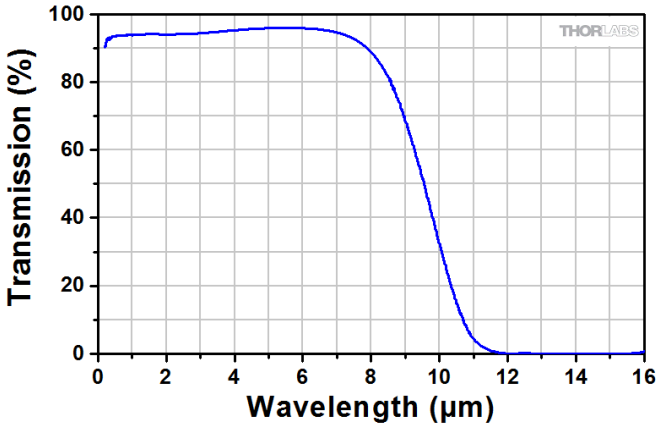

Figure 27. Transmissivity of calcium fluoride [53].

For glass wafers at low temperatures, the source literature recommends using a pyrometer with a spectral range of 8 – 14 µm and a fixed emissivity setting of 0.85. Using a pyrometer with this range would therefore ensure that the heating station is able to process both silicon and glass wafers. Given that glass becomes fully opaque to wavelengths longer than ~5 µm, filtration of the longer wavelengths should not interfere with the measurements.

A schematic illustration of the heating station incorporating each of the changes proposed above is presented in figure 28.

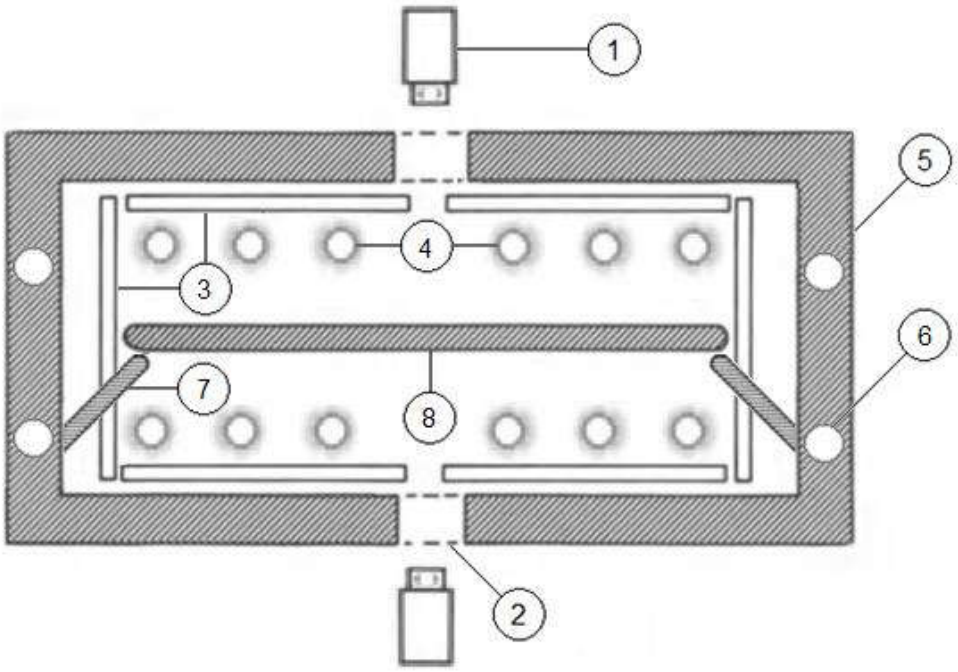

Figure 28. Schematic diagram of the heating module's revised design. The labels indicate the following parts: (1) Pyrometer with a spectral range of 8 – 14 µm, (2) Calcium fluoride window, (3) Polished aluminium reflector plate, (4) Concentric IR lamp array (tungsten-halogen in quartz tube), (5) Aluminium chamber wall, (6) Water cooling channels, (7) Wafer holding pins, (7) Wafer.

5.2 Control

To achieve a meaningful degree of control over the lamp's power output, a way to provide variable voltage to the emitters is required. This was attempted in the existing design by time-proportioning on and off periods. However, as mentioned in chapter 4.6, the control scheme was not functioning correctly, effectively reducing the heater's control into a simple on-off action.

One way to provide variable voltage without extensive changes to the tool's electrical desing is pulse-width modulation (PWM). PWM is a modulation technique in which power is switched on and off rapidly enough for the supply of power to appear continuous. By altering the relative lengths of the on and off periods, power output can be reduced to some percentage of full power. The basic principle of the technique is essentially the same as in time-proporting, but in PWM cycles are substantially shorter, in the order of milliseconds [54]. However, as electromechanical relays are incapable of switching rapidly enough to enable this and are subject to wear, they should be replaced with solid-state relays. These are semiconductor-based electrical switches without any moving parts in them, and hence capable of rapid switching.

Variable power control allows for a more sophisticated control scheme to be implemented. PI and PID controllers are typical choices for systems utilizing closed-loop feedback, including some RTP systems. In this case, PI control may be sufficient as changes in temperature to the opposite direction (i.e. cooling) are slow due to the wafer's low cooling rate in vacuum.

Modeling the radiation physics inside a rapid thermal processor with sufficient accuracy for the model to be of use in the tuning is a highly complex task and hence outside of the scope of this thesis. Thus, tuning of the control terms has to be done online using a manual tuning method.

The lack of a model also makes it very difficult to determine the effective emissivity of a wafer placed inside the chamber. Lacking a model for the wafer's effective emissivity, the correct emissivity setting for the pyrometers needs to be be determined experimentally, in a manner similar to the emissivity tests in the previous chapter.

A consideration in implementing a control scheme for the heater is the loss of heat during the transfer of the wafer from the heating station to the main process chamber. Wafer cooling rates were investigated experimentally in chapter 4.3. The rate is dependent on the initial wafer temperature, but does not exceed 1 °C/s in temperatures under 250 °C. The speed of wafer transportation, in turn, depends on the size and configuration of the wafer handling system, but typically takes no longer than 15 seconds.

To ensure that wafers are inserted into the ALD chamber in the desired temperature, the control terms should be adjusted to overshoot the target temperature by as much as the wafer is expected to cool down during transport. For example, in a case where the values presented above apply, overshoot should be 1 °C/s * 15 s = 15 °C.

6 Conclusion

The research problem addressed in this work was fairly challenging, particularly for the scope of a Bachelor's thesis.

No publications detailing a design exactly like the one discussed in this work could be found. Similar pieces of equipment presented in scientific literature had several notable differences to the design covered here, primarily that they were designed to operate at higher temperatures and that wafer heating was not the primary purpose of the designs, but a facilitating factor in another process.

Nevertheless, methodological investigation of the problem and analysis of the results with the help of scientific literature allowed for the causes of the problem to be identified.

While many of the design principles used in the examples found in the source literature were not directly applicable to the design covered in this thesis, a number features of existing RTP systems could be adapted into the new design after their function was understood.

This thesis demonstrates that a high degree of design optimization is required to create a functional heater design for a single type of substrate. It seems very difficult to design a system capable of processing the full range of available semiconductor substrates, as there seems to be no single type of temperature sensor that is suitable for all materials. The fact that the design presented in this thesis is suitable for processing of two different substrates (silicon and glass) is mostly a matter of chance. Processing other substrates such as GaAs, SiC or Ge requires the spectral properties of that substrate to be investigated and the heater's instrumentation to be adjusted accordingly.

Should it prove imperative to obtain more accurate temperature measurements than pyrometers are capable of, alternative temperature measurement methods such as fluoroptic or acoustic thermometry can be considered for future revisions of the design. While these do not suffer from the inherent problems associated with pyrometry, their implementation can be expected to be more costly and potentially bring with it a set of new problems.

References

1 McKie T. *Single-wafer processing is the key to MEMS success*. Solid State Technology [Internet]. 11/2009. Available from: https://electroiq.com/2009/11/single-wafer-processing/ [Accessed 12 February 2019].

2 Engineering360. *Semiconductor Cluster Tools Information* [Internet]. Available from: https://www.globalspec.com/learnmore/manufacturing_process_equipment/vacuum_equipment/thin_film_equipment/semiconductor_process_systems_cluster_tools [Accessed 12 February 2019].

3 Beneq. *A Thinner World* [Internet]. Available from: https://beneq.com/en/ [Accessed 15th 2019].

4 Beneq. *Beneq Coating Services.* Available from: https://beneq.com/en/thin-films/services/coating-services/introduction [Accessed 15 February 2019].

5 Beneq. *Take a Factory Tour* [Internet]. Available from: https://beneq.com/en/company/factory-tour [Accessed 15 February 2019].

6 Beneq. *Thin Film Applications* [Internet]. Available from: https://beneq.com/en/thin-films/applications [Accessed 15 February 2019].

7 LaPedus M. *ALD moves towards mainstream in IC production*. Electronic Engineering Times [Internet]. 2 February 2004. Available from: https://www.eetimes.com/document.asp?doc_id=1191960# [Accessed 15 February 2019].

8 Meriläinen, Pasi. Head of Equipment, Beneq. Personal communication. 16 January 2019.

9 Semiconductor Industry Association. *What is a Semiconductor?* [Internet] 2019. Available from: https://www.semiconductors.org/semiconductors-101/what-is-a-semiconductor/ [Accessed 4 March 2019].

10 Uesaka Y, Takei T. *Japan manufacturers react differently to chip market bounce.* Nikkei [Internet]. 10 May 2017. Available from: https://asia.nikkei.com/Business/Japan-manufacturers-react-differently-to-chip-market-bounce [Accessed 21 May 2019].

11 Birgham Young University. *Types of Wafer Substrates* [Internet]. 2018. Available from: https://cleanroom.byu.edu/EW_substrates [Accessed 4 March 2019].

12 AnySilicon. *Does Size Matter? Understanding Wafer Size* [Internet]. 23 October 2012. Available from: https://anysilicon.com/does-size-matter-understanding-wafer-size/ [Accessed 4 March 2019].

13 Glew Engineering Consulting. *Semiconductor Industry Prepares for 450mm Wafers* [Internet]. 2019. Available from: http://glewengineering.com/robotics-semiconductor-industry-prepares-for-450mm-wafers-part-2/ [Accessed 4 March 2019].

14 Rovitto M. *Electromigration Reliability Issue in Interconnects for Three-Dimensional Integration Technologies* [Internet]. Ch. 1.1.1. 1985. Available from: http://www.iue.tuwien.ac.at/phd/rovitto/node10.html [Accessed 18 April 2019].

15 Texas Instruments. *Semiconductor Manufacturing: How a Chip is Made* [Internet]. 2019. Available from: http://www.ti.com/corp/docs/manufacturing/howchip-made.shtml# [Accessed 18 March 2019].

16 Semiconductor Industry Association. *Frequently Asked Questions* [Internet]. 2019. Available from: https://www.semiconductors.org/semiconductors-101/frequently-asked-questions/ [Accessed 18 March 2019].

17 Pisarski A. *An Exploration into the World of Microprocessors.* University of Rochester [Internet]. Available from: http://www2.optics.rochester.edu/workgroups/cml/opt307/spr06/alex/index.htm [Accessed 18 March 2019].

18 Maxfield C. *How many silicon chips are there on a 300 mm wafer?* Electronic Engineering Times [Internet]. 28 June 2007. Available from: https://www.eetimes.com/author.asp?section_id=14&doc_id=1282825# [Accessed 19 March 2019].

19 Engineering 360. *Semiconductor Cluster Tools Information* [Internet]. 2019. Available from: https://www.globalspec.com/learnmore/manufacturing_process_equipment/vacuum_equipment/thin_film_equipment/semiconductor_process_systems_cluster_tools [Accessed 19 March 2019].

20 Puurunen R. *Surface chemistry of atomic layer deposition: a case study for the trimethylaluminum/water process.* Journal of Applied Physics, Vol. 97. 2005.

21 Puurunen R. *A Short History of Atomic Layer Deposition: Tuomo Suntola's Atomic Layer Epitaxy.* Chemical Vapor Deposition, Vol. 20. 2014.

22 Technology Academy Finland. *Millenium-teknologiapalkinto 2018 suomalaiselle fyysikolle – Tuomo Suntolan innovaatio mahdollistaa tietoteknisten laitteiden valmistamisen ja kehityksen* [Internet]. 2018. Available from: https://taf.fi/fi/2018/05/22/millennium-teknologiapalkinto-2018-suomalaiselle-fyysikolle-tuomo-suntolan-innovaatio-mahdollistaa-tietoteknisten-laitteiden-valmistamisen-ja-kehityksen/ [Accessed 24 April 2019].

23 Dassau E, Grosman B. Lewin D. *Modeling and Temperature Control of Rapid Thermal Processing*. Computers and Chemical Engineering. July 2005.

24 Lojek B. *Early history of rapid thermal processing.* ATMEL Corporation [Internet]. 1999. Available from: kutol.narod.ru/PUBL/rtp_otkr.pdf [Accessed 2 February 2019].

25 Roozeboom F, Parekh M. *Rapid thermal processing systems: A review with emphasis on temperature control*. Journal of Vacuum Science & Technology B, Vol. 8, No. 6. November/December 1990.

26 Sedgwick T.O. *Rapid thermal processing: how well is it doing and where is it going?* Materials Research Society Symposium Proceedings, Vol. 92. 1987.

27 Roozeboom F. *Rapid thermal processing: status, problems and options after the first 25 years.* Materials Research Society Symposium Proceedings, Vol. 303. 1993.

28 Doering R, Nishi Y, editors. *Handbook of semiconductor manufacturing technology.* 2nd edition. CRC Press. United States 2008. p. 11-4.

29 Wilson S.R. *An overview and comparison of rapid thermal processing equipment: a users viewpoint.* Materials Research Society Symposium Proceedings, Vol. 52. 1986.

30 Roozeboom F, editor. *Advances in Rapid Thermal and Integrated Processing.* Springer. Netherlands 1995. p. 30 – 31.

31 Optris. *Basic principles of non-contract temperature measurement* [Internet]. Available from: https://www.optris.com/tl_files/pdf/Downloads/Zubehoer/IR-Basics.pdf [Accessed 10th April 2019].

32 Optotherm. *Emissivity in the Infrared* [Internet]. 2018. Available from: https://www.optotherm.com/emiss-physics [Accessed 10 April 2019].

33 Edmund Optics. *The Correct Material for Infrared (IR) Applications* [Internet]. 2019. Available from: https://www.edmundoptics.com/resources/application-notes/optics/the-correct-material-for-infrared-applications/ [Accessed 15 January 2019].

34 Sato T. *Spectral Emissivity of Silicon.* Japanese Journal of Applied Physics, Vol. 6, n. 3. 1967.

35 Gelpey J, Stump P, Smith J. *Process control for a rapid optical annealing system.* Materials Research Society Symposium Proceedings, Vol. 52. 1986.

36 Sheets R. *Temperature measurement and control in a rapid thermal processor.* Materials Research Society Symposium Proceedings, Vol. 52. 1986.

37 Doering R, Nishi Y, editors. *Handbook of semiconductor manufacturing technology.* 2nd edition. CRC Press. United States 2008. p. 11-38.

38 Sopori B, Chen W, Madjdpour J, Ravindra N. *Calculation of emissivity of Si wafers.* Journal of Electronic Materials, Vol. 28. 1999.

39 Fraden J. *Handbook of Modern Sensors: Physics, Designs, and Applications.* 2nd edition. United Kingdom 2010. Springer. p. 561.

40 LumaSense Technologies. *Fluoroptic Temperature measurement* [Internet]. 2018. Available from: https://www.lumasenseinc.com/EN/products/technology-overview/our-technologies/fluoroptic/fluoroptic-temperature-measurement.html [Accessed 29 April 2019].

41 Nulman J, Cohen B, Blonigan W, Antonio S, Meinecke R, Gat A. *Pyrometric temperature measurements and compensation in an RTP chamber.* Materials Research Society Symposium Proceedings, Vol. 146. 1989.

42 Choi JY, Do HM. *A Learning Approach of Wafer Temperature Control in a Rapid Thermal Processing System.* IEEE. 2001.

43 Wacher A, Seymour B. *A radiation Model of a Rapid Thermal Processing System.* Mathematics-in-Industry Case Studies Journal, Vol. 3. 2011.

44 National Physical Laboratory. *What do 'high vacuum' and 'low vacuum' mean? (FAQ – Pressure)* [Internet]. 9 August 2007. Available from: http://www.npl.co.uk/reference/faqs/what-do-high-vacuum-and-low-vacuum-mean-(faq-pressure) [Accessed on 1 March 2019].

45 Valkealahti, Veli. Product Manager, Sarlin Oy. Personal communication. 21 January 2019.

46 Schneider Electric. *Principles of PID Control and Tuning* [Internet]. 2009. Available from: https://www.eurotherm.com/principles-of-pid-control-and-tuning [Accessed 5 March 2019].

47 Doering R, Nishi Y, editors. *Handbook of semiconductor manufacturing technology.* 2nd edition. CRC Press. United States 2008. p. 11-31.

48 Williamson. *Industrial Infrared Pyrometers* [Internet]. Available from: https://www.williamsonir.com/wp-content/uploads/2018/06/2018-Product-Overview-Brochure.pdf [Accessed 5 March 2019].

49 LumaSense Technologies. *LumaSense Impac Pyrometers* [Internet]. Available from: https://www.lumasenseinc.com/uploads/Products/Temperature_Measurement/Infrared_Thermometers/IMPAC_Pyrometers/pdf_IMPAC_pyrometers/EN-IMPAC-Pyrometers_Overview-Brochure.pdf [Accessed 5 March 2019].

50 Wen CD, Mudawar I. *Emissivity characteristics of roughened aluminium alloy surfaces and assessment of multispectral radiation thermometry (MRT) emissivity models.* International Journal of Heat and Mass Transfer, Vol. 47. 2004.

51 Delateur M. *Semiconductor contamination: Not your usual suspects.* EDN Network [Internet]. 2 April 2008. Available from: https://www.edn.com/electronics-news/4325260/Semiconductor-contamination-Not-your-usual-suspects [Accessed 30 April 2019].

52 Maturilli A, Helbert J. *Characterization, testing, calibration and validation of the Berlin emissivity database.* Journal of Applied Remote Sensing, Vol. 8. 2014.

53 Thorlabs. *Calcium fluoride windows* [Internet]. 2019. https://www.thorlabs.com/NewGroupPage9.cfm?ObjectGroup_ID=3978 [Accessed 5 May 2019].

54 Heath J. *PWM: Pulse Width Modulation: What is it and how does it work?.* Analog IC Tips [Internet]. 4 April 2017. Available from: https://www.analogictips.com/pulse-width-modulation-pwm/ [Accessed 4 May 2019].